REPORT DOCUMENTATION PAGE

Form Approved
OMB NO. 0704-0188

1. AGENCY USE ONLY (Leave Blank)	2. REPORT DATE	3. REPORT TYPE AND DATES COVERED
		Final Progress Report 1, April, 2000 - 31, March, 2002

4. TITLE AND SUBTITLE
Chemistry Of Destroying Of Organophosphorus Compounds In Flame And Mechanism Of Their Action As Fire Suppressants

5. FUNDING NUMBERS
DAAD 19-00-1-0136 Modification No. P00001

6. AUTHOR(S)
Korobeinichev, O.P. Shmakov A.G.
Shvartsberg, V.M. Bolshova, T.A.
Chernov A.A.
Mamaev, A.L.
Sokolov, V.V.

7. PERFORMING ORGANIZATION NAME(S) AND ADDRESS(ES)
Institue of Chemical Kinetics & Combustion Russian Academy of Sciences
3, Institutska st. Novosibirsk, 630090 Russia

8. PERFORMING ORGANIZATION REPORT NUMBER

9. SPONSORING / MONITORING AGENCY NAME(S) AND ADDRESS(ES)
U. S. Army Research Office
P.O. Box 12211
Research Triangle Park, NC 27709-2211

10. SPONSORING / MONITORING AGENCY REPORT NUMBER

11. SUPPLEMENTARY NOTES
The views, opinions and/or findings contained in this report are those of the author(s) and should not be construed as an official Department of the Army position, policy or decision, unless so designated by other documentation.

12 a. DISTRIBUTION / AVAILABILITY STATEMENT
Approved for public release; distribution unlimited.

12 b. DISTRIBUTION CODE

13. ABSTRACT (Maximum 200 words)

The structure of atmospheric lean (φ=0.8) and rich (φ=1.2) $CH_4/O_2/Ar$ and $C_3H_8/O_2/Ar$ flames doped with trimethylphosphate (TMP) was studied by molecular beam mass spectrometry (MBMS) and modeling. Methodic difficulties of MBMS measurement of the structure of atmospheric flames were analyzed and recommendations were elaborated. An influence of TMP additive on the structure of atmospheric flames was demonstrated. A strong influence of equivalence ratio of a flame on the concentration of PO, PO_2, HOPO, $HOPO_2$ and $OP(OH)_3$ has been observed. The influence of TMP additive on concentration of H, OH, CH_3 was investigated. TMP loading dependencies of burning velocity of a stoichiometric CH_4/air and C_3H_8/air flames were measured and simulated. TMP and triethylphosphate loading dependence of normalized extinction strain rate of opposed-jet $CH_4/O_2/N_2$ flame was measured. Both OPC demonstrated close fire suppression effectiveness. Comparison of the experimental data with results of modeling on flame structure and burning velocity made it possible to reveal essential drawbacks of our kinetic model proposed early and noticeably refine it. The published models of Glaude et al. and Babushok and Tsang were tested by comparing measured and simulated concentrations of phosphorus containing flame species. In order to make the mechanism to predict better both the flame structure and burning velocity rate constants of eight the most important reactions from Twarowski mechanism have been modified. The possible reasons of the failure of the models to predict the structure of the rich flames were analyzed and perspectives of future research were discussed.

14. SUBJECT TERMS	15. NUMBER OF PAGES
	16. PRICE CODE

17. SECURITY CLASSIFICATION OR REPORT	18. SECURITY CLASSIFICATION ON THIS PAGE	19. SECURITY CLASSIFICATION OF ABSTRACT	20. LIMITATION OF ABSTRACT
UNCLASSIFIED	**UNCLASSIFIED**	**UNCLASSIFIED**	**UL**

CONTENTS

List of publications:

(a) Manuscripts submitted, but not published

1. Korobeinichev, O.P., Bolshova, T.A., Shvartsberg, V.M., Shmakov, A.G. Study of Inhibition Effect of Organophosphorus Compounds on Structure of Laminar Premixed Atmospheric $C_3H_8/O_2/Ar$ Flames and Burning Velocity of Stoichiometric Propane/Air mixtures, Twenty-Ninth Symposium (International) on Combustion 2002, submitted for publication.
2. Korobeinichev, O.P., Chernov, A.A., Sokolov, V.V., Krasnoperov, L.N. Kinetics of the Destruction of Organophosphorus Compounds in Corona Discharge. 2002, accepted for publication in Journal "Chemical Physics" (in Russian).
3. Korobeinichev, O.P., Chernov, A.A., Sokolov, V.V., Shvartsberg, V.M., Bolshova, T.A., Krasnoperov, L.N. Kinetics of Destruction of Diisopropyl Methylphosphonate in Corona Discharge, Accepted for publication in International Journal of Chemical Kinetics (proof has been corrected).
4. Korobeinichev O.P., Bolshova T.A., Shvartsberg V.M., Shmakov A.G. Inhibition effect of organophosphorus compounds on structure of atmospheric $C_3H_8/O_2/Ar$ and $CH_4/O_2/Ar$ flames. In: Proceedings, Halon Options Technical Working Conference, 2002. Accepted as oral presentation.
5. Shmakov A.G., Korobeinichev O.P., Bolshova T.A., Shvartsberg V.M, Knyazkov D.A., Zakharov L.S., Kudravtsev I.U., Furin G.G. Study of effect of organophosphorus fire suppressants on premixed C_3H_8/Air and diffusive counterflow CH_4/Air flames. In: Proceedings, Halon Options Technical Working Conference, 2002. Accepted as oral presentation.

(b) Papers published in peer-reviewed journals

1. Korobeinichev, O.P., Ilyin, S.B., Bolshova, T.A., Shvartsberg, V.M and Chernov, A.A., "The Destruction Chemistry of Organophosphorus Compounds in Flames – III: The Destruction of DMMP and TMP in a Flame of Hydrogen and Oxygen," Combustion and Flame 121 (2000) pp. 593-609.
2. Korobeinichev, O.P., Chernov, A.A., Bolshova, T.A., "Destruction of Organophosphorus Compounds in Flames IV: Destruction of DIMP in a Flame of $H_2 + O_2 + Ar$" Comb . Flame 123: #3, pp.412-420 (2000).
3. Korobeinichev, O.P., Bolshova, T.A., Shvartsberg, V.M., and Chernov, A.A. "Inhibition and Promotion of Combustion by Organophosphorus Compounds Added to Flames of CH_4 or H_2 in O_2 and Ar", Combustion and Flame 124: (2001).
4. Korobeinichev, O.P., Shvartsberg, V.M., Bolshova, T.A., , Shmakov, A.G., Knyazkov, D.A. Inhibition of Methane-Oxygen Flames by Organophosphorus Compounds, Combust. Explos. and Shock Waves 38: 2, pp. 3-10 (2002).

(c) Papers published in non-peer-reviewed journals or in conference proceedings

1. Korobeinichev, O., Mamaev, A., Sokolov, V., Bolshova, T., and Shvartsberg V.. Inhibition of Methane Atmospheric Flame by Organophosphorus Compounds. In: Proceedings, Halon Options Technical Working Conference, 2000, pp. 164-173.
2. Korobeinichev, O.P., Mamaev, A.l., Bolshova, T.A., Shvartsberg, V.M. Mechanism of Inhibition of $CH_4/O_2/Ar$ flames by Phosphorus-containing Compounds. XII Symposium on Combustion and Exposition, September 11-15, 2000, Chernogolovka, Russian Academy of Sciences. Poster presentation. Proceedings, Part 1, pp. 86-88 (in Russian).
3. Korobeinichev, O.P., Mamaev A. Sokolov V.V., Bolshova, T.A., Shvartsberg, V.M., Zakharov L.S., Kudravtsev I.Yu., Experimental Study and Modeling of the Effect of Phosphorous-Containing Compounds on Premixed Atmospheric Methane-Oxygen Flame

Structure and Propagation Velocity - In: Proceedings, Halon Options Technical Working Conference, Albuquerque, NM, 2001, pp. 173-186.

(d) Papers presented at meetings, but not published in conference proceedings

1. Korobeinichev, O.P., Chernov, A.A., Sokolov, V.V., Krasnoperov, L.N. Destruction of Chemical Warfare Agents Stimulants. in Corona Discharge. All-Russian Conference on Chemical Demilitarization. CHEMDET 2000, oral presentation, Book of Abstracts, pp. 37-39 (in Russian).
2. Korobeinichev, O.P., Chernov, A.A., Sokolov, V.V., Krasnoperov, L.N. Kinetics of the Destruction of Organophosphorus Compounds in Corona Discharge. 16-th International Symposium on Gas Kinetics, July 23rd - 27th, 2000, Cambridge, UK, poster presentation. Book of Abstracts.PC 15.
3. Korobeinichev, O.P., Chernov,A.A., Sokolov**,** V.V**.,** Kinetics of Destruction of Organophosphorous Compounds in Corona Discharge**,** Fifth International Conference on Chemical Kinetics, Gaithersburg, Maryland USA, July 16-20, 2001, *Abstracts of papers*, pp.197-198. Available at www.nist.gov/kinetics2001

Scientific personnel

Professor Oleg P. Korobeinichev
Dr. Vladimir M. Shvartsberg
Dr. Andrey Shmakov
Dr. Anatoly A. Chernov
Tatyana A. Bolshova
Alexey L. Mamaev
Vladimir V. Sokolov
Denis Knyazkov
Vladimir Shvartsberg has defended his PhD thesis "Structure of $H_2/O_2/Ar$ and $CH_4/O_2/Ar$ subatmospheric flames doped with trimethylphosphate".
Anatoly Chernov has defended his PhD thesis "Study of Flame Structure of Solid Propellants Based on Ammonium Perchlorate and Polybutadiene Binder".
Andrey Shmakov has defended his PhD thesis "Study of Kinetics and Mechanism of Thermal Decomposition of Ammonium Dinitramide and Glycydilazide Polymer by Method of Dynamic Mass Spectrometry"

“Report of inventions”
No

STATEMENT OF THE PROBLEM STUDIED

The investigations performed during the granted period were aimed at understanding of the processes of inhibition of combustion of methane and propane flames by organophosphorus compounds (OPC), which are known to be perspective ecologically safety fire suppressants. Molecular beam mass spectrometry (MBMS) and computer modeling were shown to the most effective technique to study the structure of $CH_4/O_2/Ar$ and $C_3H_8/O_2/Ar$ flames doped with trimethylphosphate (TMP) and stabilized on a flat burner at 1 atm. The foreground task of experiment was to measure profiles of temperature and concentration of stable and labile species: free atoms and radicals and phosphorus-containing products of TMP destruction in flames PO, PO_2, HOPO, $HOPO_2$ and $OP(OH)_3$, which are responsible for inhibition process. OPC loading dependence of burning velocity of atmospheric CH_4/air and C_3H_8/air flames was planned to be measured using Mache-Hebra nozzle burner and total area method of a flame image. Comparing the experimental data with modeling results and applying sensitivity analysis of the kinetic model for TMP destruction elaborated earlier was planned to be refined. Finally the refined kinetic model must predict both burning velocity and chemical structure of an atmospheric flame. Fire suppression effectiveness of OPC for premixed methane flame stabilized on opposed-jet burner was planned to be studied.

`Scientific Progress and Accomplishments

INTRODUCTION

Intensive study of destruction chemistry of organophosphorus compounds (OPC) began about 10 years ago and was associated mainly with a problem of chemical warfare agents (CWA) disposal as incineration was recognized to be the basic technology for CWA disposal in USA. The first results were obtained in USA and Russia practically simultaneously and were devoted to the study of structure of H_2/O_2/Ar flames doped with dimethyl methylphosphonate (DMMP) stabilized on a flat burner at a pressure of about 50 Torr using molecular beam mass spectrometry (MBMS) with soft ionization by electron impact [1,2] and vacuum ultraviolet [3]. Kinetic model for DMMP destruction in a flame was proposed by Werner and Cool [3] and was based on qualitative results on structure of H_2/O_2/Ar flame doped with DMMP [3] and thermochemical and kinetic data of C. Melius calculations [4] for the stages involving DMMP and phosphorus-containing intermediate products of it destruction. To describe the interaction of final phosphorus-containing products with H and OH radicals Twarowski mechanism [5,6,7] was applied. Comprehensive study of H_2/O_2/Ar [8-11] flames doped with OPC (trimethyl phosphate (TMP) and DMMP) and stabilized on flat burner at low pressure was performed by the authors and resulted in development of kinetic mechanism [10,12]. The model [10,12] adequately described experimental data on concentration profiles of stable and labile flame species including radicals H, O, OH, PO, PO_2 and other phosphorus-containing species (PCS) HOPO, $HOPO_2$, $OP(OH)_3$ at low pressure.

Recently after signing Montreal Protocol forbidding production of Halon 1301 and search of candidates for its replacement OPC attracted attention as fire suppressants and the need of study of mechanism of action of OPC on combustion has emerged. In connection with this problem the mechanism of action of OPC additives on low pressure and atmospheric hydrocarbon flames was studied. Structure of methane premixed laminar flat flames was studied using MBMS and computer modeling [12-15]. Methane opposed-jet flames were studied using laser induced fluorescence and computer modeling [16]. Effectiveness of number of OPC as fire suppressants was determined using cup-burner technique [17]. The investigations [14,15] revealed the drawbacks of early proposed mechanism of OPC action and all efforts were exerted for its refinement. The investigations of Glaude et al [18,19] were devoted to the development of mechanisms of OPC destruction in flow reactor and in flames. Comparison of calculated data obtained with experimental results on structure of low pressure

H_2/O_2/Ar flame doped with DMMP and TMP demonstrated satisfactory agreement not only for stable flame species but also for labile PCS such as PO, PO_2, HOPO and $HOPO_2$ [18].

Babushok and Tsang [20,21] proposed another kinetic mechanism for DMMP destruction in CH_4/air atmospheric flame. This mechanism was applied for calculation of burning velocities of stoichiometric CH_4/air flame at atmospheric pressure.

In spite of significant progress in study of combustion chemistry of OPC there is a deficit of quantitative experimental data on flame structure, which are needed for further refinement of a mechanism of action of OPC on combustion. Besides, the above-mentioned models were applied to simulate only a several experimental data on flame structure and burning velocity. The goal of present research was to improve our understanding of OPC combustion chemistry and the inhibition mechanism through experimental and modeling study of structure and velocity of propagation of atmospheric C_3H_8/O_2/Ar flames doped with TMP.

EXPERIMENTAL

Experimental Conditions

To investigate OPC effect on the structure of atmospheric flames four following flames have been chosen:

Table 1

COMPOSITION (in mole fractions)			Equivalence
CH_4	O_2	Ar	ratio (φ)
0.06	0.15	0.79	0.9
0.075	0.125	0.80	1.2
C_3H_8	O_2	Ar	
0.025	0.136	0.839	0.9
0.029	0.121	0.85	1.2

The flames were stabilized on a flat Botha-Spolding type burner 16 mm in diameter at atmospheric pressure and temperature 370-400 K. Combustible mixture was prepared with a help of mass flow controllers (MKS Instruments Inc., model 1299S). Total volumetric flow rate was 1.5 slpm. OPC was added to a combustible mixture flow using saturator with liquid TMP in controlled temperature bath.

Methodic problems Development of MBMS Technique for Atmospheric Flames.

During experimental study it has been found out that the time of exploitation of quartz probes is much shorter in atmospheric flames than in low pressure flames. It occurs because

of 2 reasons. The first one is explained by higher temperature of a probe in atmospheric flame due to more effective thermal contact between a flame and a probe at atmospheric pressure. When quartz is heated above 1200^0C and kept at the temperature for the prolonged time it starts crystallizing. This process is accelerated by contamination of the surface and is followed a quartz probe destruction. Besides, while sampling the phosphorus compounds form a solid film of pyrophosphoric acids (especially near the tip of the probe) which alloys with heated quartz to form easily melted phosphate glass.

The systematic research of chemical structure of gaseous flames at 1 atm using MBMS was not performed in the past. It may be explained mainly by methodical difficulties in taking into account the appreciable perturbations of the flames caused by a sonic probe When studying the structure of atmospheric flat flames using molecular beam mass spectrometry (MBMS) it has been discovered that measured concentration profiles of main flame species CH_4, O_2 and H_2O are displaced from the temperature profile. These profiles are. shifted in accordance with the shift of lines of equal concentrations [22] in a flame caused by a probe It is explained by appreciable heat losses from the flame not only into the burner but into a probe and surrounding space. The flame heat losses into the probe depend on the probe's position relatively the burner and can not be estimated.

To measure temperature profile of the perturbed flame correctly one should use a thermocouple placed near the probe's tip. This technique was proposed by two groups of authors [23,24] and was applied for flat flames stabilized at low pressure. Earlier [25] we have demonstrated that for the probes having the wall thickness 0.05 mm the temperature profiles in low pressure flames measured by a thermocouple near the probe's tip and far off probe practically do not differ from one another. The authors [23,24] recommend to a place a thermocouple at the distance of 2-3 diameter of the thermocouple's junction from the probe that is 0.2-0.3 mm in the case of the thermocouple 0.1 mm in diameter. At atmospheric pressure when the effect of a probe on the flame is rather stronger the selection of optimal distance between a probe and a thermocouple was performed by comparison of concentration profiles of CH_4, O_2 and H_2O with profiles of temperature measured by a thermocouple which junction was placed at varied distances δ from the probe's tip. Figures 1, 2 and 3 demonstrate a perturbation of the flat atmospheric methane lean and rich flames with additive and without its by a sonic probe. Comparing the temperature profiles (Figs. 1-2) obtained with a help of thermocouple placed at various distances from the tip of the probe one can see that the probe decreases final flame temperature for about 200 K and noticeably increases the width of a

combustion zone. It is noteworthy that the concentration profiles should be moved towards the burner on the value of sampling shift [22]. The goal of the comparison is to achieve the similarity of profiles of concentrations of stable flame species and temperature. The experiments demonstrated optimal distance to be $\delta=0.3\pm0.03$ mm for above flames and probe used. It is evidently that this recommendation can be applied for certain types of probes and flame.

Temperature Measurements

The temperature of the flames was measured by a Pt - Pt+10 % Rh thermocouples welded from wire of 0.02 mm in diameter. The thermocouple covered by a layer of SiO_2 was 0.03 mm in diameter. The thermocouple had a Π-shape with shoulders about 2 mm long. At such ratio wire diameter/shoulder length the heat losses in the cold ends of a thermocouple are negligibly small.

To verify the accuracy of measurement of temperature profile and estimation of the sampling shift the method of pneumatic probe [26] was applied to measure the temperature profiles in the flames. The temperature profile obtained using this technique satisfactorily coincided with that measured by a thermocouple placed at the distance of 0.3 mm from the probe's tip for above mentioned flames and probe. But for another probe the temperature profile obtained using the method of pneumatic probe satisfactorily coincided with that measured by a thermocouple placed at the distance of 0.6-0.7 mm from the probe's tip (Fig 4). Actually a pneumatic probe determines the averaged temperature in the sampling area. Therefore, the congruence of temperature profiles measured using both techniques confirms a correctness of the distance between a thermocouple and the probe, which was chosen for measuring flame temperature. Besides it is necessary to note that modeling data justified the similarity of profiles of temperature and species concentrations in flame. Accordingly to the data of modeling of structure of $C_3H_8/O_2/Ar$ flame stabilized on the flat burner, concentration profile of H_2O is similar to temperature profile (Fig. 5). Thus, regularity of the choice of the "proper" temperature profile was confirmed also by the similarity of the above temperature profile and measured concentration profile of O_2.

Experimental Setup

The quadrupole mass spectrometer with a molecular beam sampling system has been partially described previously [2,8] For the current experiments, the geometry of the sampling system was as follows: probe - skimmer distance - 20 mm, probe - collimator distance - 320 mm, probe - ion source distance - 390 mm. Stage 1 was

pumped by an oil diffusion pump (2000 l/s), which provided a working pressure of 5×10^{-4} Torr. Stages 2 and 3 were pumped with a turbomolecular pump (500 l/s), which maintained pressures of about 10^{-5} Torr (stage 2) and 2×10^{-8} Torr (stage 3) during the experiments. The MS 7302 quadrupole mass spectrometer, produced by the Experimental Plant of the Russian Academy of Sciences, was equipped with a modernized ion source with a small spread of electron energy, corresponding only to the thermal spread [27,28]. In practice, ionization potentials were measured e.g., of argon and oxygen with an accuracy of ± 0.2 eV. This ion source allowed operation at low ionization energies (IE) close to the ionization potentials of the atoms, radicals and molecules investigated. The molecular beam was chopped (frequency 33-49 Hz) and a photodiode signal was used as a base signal in the measurements of the modulated component of the molecular beam. The measurements were made under ion counting conditions by CAMAC apparatus and a computer. The power supply for the chopper motor was computer-controlled and the rotation frequency was defined with a timer. The photodiode signal passed through a phasor, which initiated the time interval for the gated pulse counter to operate. The pulsed signal from the electron multiplier was amplified and then passed to the pulse counter. The base frequency of 1 MHz for the timers was produced by a generator. The ionization energy of electrons was controlled by a digital-to-analog converter with a stability of ± 0.005 V. To determine the reliability of the measured concentrations and their reproducibility, each one was deduced from 4 to 6 measurements. The measurements usually did not last more than 12 s. A mean-square error was estimated; only those peak intensities with mean-square errors of less than 35% were used.

Burning Velocity Measurement

Study of OPC additives on burning velocity of flames was performed using Mache-Hebra nozzle burner described elsewhere [29] and the total area method from a flame image. Burning velocity was estimated as u=W/S, where W - volumetric flow rate of the combustible mixture, S - area of the flame cone. Accuracy of measurement of burning velocity was about 4%. Experimental technique was described earlier [15].The size of the flame cone was measured by luminous zone but not with a help of schlieren method. This technique introduced an error in absolute values of burning velocity. That is why here we present the

ratio (**f**) of burning velocity of inhibited flame (u_g) to burning velocity of undoped flame (u_0) as a value characterizing the effectiveness of an inhibitor. To ascertain in reliability of the data obtained magnitude of **f** was measured in different way. For that the height of the cone of doped flame was decreased and became equal the cone of a undoped flame owing to decrease of volumetric flow rate of the combustible mixture. In this case effectiveness of an inhibitor was estimated as $\mathbf{f}=W_g/W_o$, where W_g and W_0 are the volumetric flow rate of combustible mixture for inhibited and for uninhibited flames correspondingly. Results obtained by both methods demonstrated satisfactory coincidence.

MODELING

PREMIX and CHEMKIN-II codes [30,31] were used for simulation of concentration profiles and burning velocity. Simulation of flat flame structure was performed using specified experimentally measured profiles of temperature. A number of kinetic models for oxidation of methane are available (see Table 2). The simplest one involves 18 species in 59 stages. This mechanism involves only C_1 hydrocarbons and is incorporated in PREMIX and CHEMKIN II software package [30,31]. Besides, there are 2 models [32,33] for methane oxidation, which involves C_1-C_3 species.

Table 2. Brief Characteristics of Mechanisms for Hydrocarbon Oxidation.

Mechanism	Number of		C-containing species	Number of N-containing species
	stages	species		
CHEMKIN [30,31]	58	18	C_1	0
GRI 3.0 [32]	325	53	C_1-C_3	8
Leeds [33]	175	37	C_1- C_4	0
Konnov [34]	1200	127	C_1-C_4, C_6	35

For study of C_3H_8/O_2/Ar flames at atmospheric pressure the mechanism based on Konnov's detailed reaction model [34] for combustion of small hydrocarbons was used. This mechanism involves 127 species containing H, O, C, N elements and 1200 elementary reactions. Mechanisms for destruction of TMP and DMMP in H_2/O_2/Ar and CH_4/O_2/Ar flames stabilized on a flat burner at low pressure of 47-76 Torr was elaborated earlier [10,12,14]. The model comprises 14 stages for destruction of TMP and organophosphorus intermediates, 5 stages for destruction of orthophosphoric acid, and 15 stages of so-called reduced Twarowski mechanism [5,6,7], which were modified by us [10,12]. Later these models were applied to simulate the structure and burning velocity of atmospheric flames. To

obtain a satisfactory agreement between experimental and modeling results a number of rate constants were modified.

One of the kinetic models for OPC destruction in a flame describing inhibition effect of OPC on combustion, which was used to simulate the flame structure, was the mechanism proposed by Glaude et al [18,19]. A kinetic model of DMMP and TMP destruction in a flame includes 202 reactions involving 41 phosphorus-containing species (PCS). The authors evaluated rate constants of many reactions. Rate constants of the reactions from Twarowski mechanism have been evaluated too. Another mechanism proposed by Babushok and Tsang [20,21 comprises 24 stages with participation of OPC from the model of Werner and Cool [3], 79 reactions from Twarowski mechanism (including reactions of phosphine oxidation with participation of PH_3, PH_2, PH) and number of stages of interaction of CH_3 and CH_3O with phosphorus oxides. It should be noticed that our kinetic model for OPC destruction as well as the model proposed by Babushok and Tsang are based mainly on thermochemistry estimated by C. Melius [4]. The model elaborated by Glaude et al. has thermochemical data estimated by the authors.

Structure of CH_4/O_2/Ar Flames

Figure 6 demonstrated experimental temperature profiles in the lean CH_4/O_2/Ar flame doped with 350 ppm and without additive. The measurements were performed using a thermocouple placed away from the probe. As can be seen, in the presence of TMP the width of the combustion zone increases (i.e. the additive inhibits combustion) and the final temperature in the post-flame zone is slightly higher. Visual observations demonstrate that the flame turns orange and a distance between the burner and luminous front increases.

Thermocouple measurements showed that the profiles obtained by a thermocouple placed at the distance 0.1-0.3 mm from the tip of a microprobe are almost identical to those of unperturbed flame. It indicates that the microprobe introduces minor thermal perturbations into the flame.

The temperature of the burner surface was additionally measured by a thermocouple embedded into the center of the burner's filter. The temperature of the burner surface was demonstrated to be the same for both undoped flames - nearly 400K. For the doped flames where the preflame zone is increased in comparison with uninhibited flames the temperature is 370K. The influence of a probe on the temperature of the surface is insignificant (within 2-3K).

Figure 7 shows the effect of 350 ppm of TMP on concentration profiles of CH_4, O_2 and H_2O in the lean $CH_4/O_2/Ar$ flame obtained using the microprobe sampling. The profiles in Fig. 7 are presented with a sampling shift Δz=0.4 mm. The fact that the value Δz was determined correctly is supported by a satisfactory similarity of temperature (Fig. 6) and the concentration profiles (Fig. 7). It is obvious that an addition of TMP increases the width of the zone for CH_4, O_2, and H_2O. A satisfactory agreement between simulated and measured concentration profiles presented in Fig. 7 is observed.

The structure of the lean $CH_4/O_2/Ar$ flame doped with 2200 ppm of TMP and without additive was studied by MBMS. Figure 8 shows simulated and measured concentration profiles of CH_4, O_2 and H_2O and experimental profile of temperature in the lean undoped flame. Here and below all concentration profiles are shifted towards the burner surface for the value of sampling shift [22]. The sampling shift (z) according to [22] depends on the flame temperature as $\Delta z = z_0(T_0/T)^{0,5}$ where T_0 - is initial temperature of the combustible mixture, T - is a flame temperature for a certain distance from the burner, z_0 - sampling shift at $T=T_0$ [22]. In present study the sampling shift varied from 0.51-0.27 mm. A comparison shows the results of simulation to be in a satisfactory agreement with experimental data. This fact, in particular, confirms a validity of this approach for study of flame structure at a pressure of 1 atm.

Figure 9 demonstrates simulated and measured concentration profiles of CH_4, O_2, H_2O, CO and CO_2 and measured profile of temperature in the lean flame doped with 2200 ppm of TMP. An agreement between modeling and experimental data is observed.

In Figures 10 and 11 concentration profiles of CH_4, O_2, and H_2O and measured profiles of temperature in the rich $CH_4/O_2/Ar$ flame without additive and in that doped with 2200 ppm of TMP are shown correspondingly. As it is seen in Figs. 10 and 11, the additive increases the combustion zone width of the flame for about 0.4 mm. The increase of combustion zone results in decrease of the temperature gradient near the burner surface that in its turn reduces the heat losses from the flame into the burner. That is why the inhibited flames are perturbed much stronger by a probe than uninhibited ones. Finally it results in appreciable obstacles in reproducing the experimental results obtained using different probes. The use of a probe with just the same characteristics (wall thickness, diameter of orifice) can help to overcome these difficulties. The simulated concentration profiles of CH_4, O_2, H_2O in these flames are presented in Figs. 10 and 11. Comparison of experimental and modeling results reveals a satisfactory agreement.

Concentration profiles of TMP and phosphorus-containing products of its destruction in the lean $CH_4/O_2/Ar$ flame doped with 2200 ppm PO, PO_2, HOPO, $HOPO_2$ and $OP(OH)_3$ are shown in Fig. 12. The energy of ionizing electrons of 12.8 eV for PO, PO_2 and HOPO, 14.5 eV for $HOPO_2$ and 17.5 eV for $OP(OH)_3$ made it possible to use the calibration coefficients for the species obtained earlier [8]. The molecular ion $HOPO_2^+$ and fragmentary ions of TMP and some intermediate products of TMP destruction in flames such as dimethylphosphate, dimethylphosphite and others contribute in the peak at 80 amu measured at energy of ionizing electrons of 14.5 eV As appearance potentials of fragmentary ions of OPC are lower than ionization potential of $HOPO_2$ it is impossible to escape contribution of fragmentary ions into peak at 80 amu. To obtain concentration profile of $HOPO_2$ it is necessary to subtract the contribution all OPC - intermediates of TMP destruction in flame in intensity of peak at 80 amu. Unfortunately, it is impossible as mass spectra of some of the intermediates (methylphosphate, methylphosphite and others) are unknown because of their instability and therefore inaccessibility at normal conditions. Taking into account the contributions in peak at 80 amu from TMP and dimethylphosphate (peak at 126 amu), assuming absence of the contributions into this peak from other OPC intermediates and considering the concentration profile to be smooth and relying on equation of conservation on phosphorus, the profiles of concentrations of $HOPO_2$ in the lean and rich $CH_4/O_2/Ar$ flames were plotted in Figs. 12 and 13. So, Figures 12 and 13 represent final concentration of $HOPO_2$ in the flames reliably only at 4 mm from the burner surface where there are no OPC. Concentration profiles of PO, PO_2, HOPO, $HOPO_2$ and $OP(OH)_3$ in the rich $CH_4/O_2/Ar$ flame doped with 2200 ppm of TMP are presented in Fig 12. Orthophosphoric acid is an intermediate product of TMP destruction in the rich flame. It may be explained by relatively high final temperature of the flame. Unlike the lean flame in the rich one the main final phosphorus-containing compound is HOPO. One can notice that the width of reaction zone of phosphorus-containing species is larger than that of stable species (CH_4, O_2, H_2O) especially in the lean flame. Simulated profiles of concentration of PO, PO_2, HOPO, $HOPO_2$ and $OP(OH)_3$ in the lean and rich flames are presented in Figs. 12 and 13 correspondingly. Considering difficulties emerging at measuring concentration of these species and accuracy of determination of their calibration coefficients [8] one can observe a satisfactory agreement between experiment and modeling for the lean flame. The structure of this flame was simulated using 2 published kinetic models describing the action of OPC on combustion. The first one elaborated by Glaude et al. [18,19] is defined as mechanism 2, and the second one proposed by Babushok and Tsang [20,21] is defined as mechanism 3. The calculated final

concentrations of PO, PO_2, HOPO, $HOPO_2$ and $OP(OH)_3$ in the lean and rich $CH_4/O_2/Ar$ flames doped with 2200 ppm of TMP are presented in Tables 3 and 4.

TABLE 3. Fraction of number of moles of a phosphorus-containing compound in total number of moles of PCS (in %) in post-flame zone of the lean $CH_4/O_2/Ar$ flame calculated using 3 different mechanisms, equilibrium state and measured experimentally

Species	Mole fractions			Equilibrium concentrations at 1685 K	Experimental results Range
	1	2	3		
PO	0.0	0.0	0.4	0.0	0 - 0.6
PO_2	10.6	0.5	37.7	1.0	1 - 5
HOPO	8.3	1.5	7.7	0.6	4.8 - 8.8
$HOPO_2$	74.3	96.6	47.5	90.6	58 - 100
$PO(OH)_3$	6.8	0.6	4.4	7.8	4.5 - 13.5

TABLE 4. Fraction of number of moles of a phosphorus-containing compound in total number of moles of PCS (in %) in post-flame zone of the rich flame $CH_4/O_2/Ar$ (0.075/0.125/0.80) calculated using 3 different mechanisms, equilibrium state and measured experimentally (L=4 mm)

Species	Mole fractions			Equilibrium concentrations at 1800K	Experimental results Range
	1	2bab	3 gloud		
PO	4.2	5.7	0.0	1.2	1.9÷9.5
PO_2	8.1	25.3	6.7	7.0	2.2÷11.0
HOPO	60.7	60.3	52.8	82.9	62.6÷93.8
$HOPO_2$	26.1	8.3	34.7	8.6	6.6÷12.1
$PO(O)_3$	1.0	0.3	0.1	0.3	0.0

Final concentrations of phosphorus-containing species in the flame calculated using our model (mechanism 1) are shown in Tables 3 and 4 together with experimental data and results of calculations of the equilibrium concentrations of these species at final flame temperature using thermochemic data accepted in mechanism 1.. Comparison of modeling data with experiment revealed that all three models provide a satisfactory agreement with

approximately the same deviation for final concentrations of phosphorus-containing species in the lean flame. Comparison of the results of thermodynamic calculations with those of experiment and modeling demonstrated a distinction between them. It indicates that thermodynamic equilibrium in these conditions is not achieved. Only concentrations of some of these phosphorus-containing compounds are close. It can be expected considering overequilibrium concentration of H and atoms and OH radicals, which react with phosphorus-containing species producing the inhibition effect. Calculation of the equilibrium compositions involving all species from mechanism 3 gave the same results. Thermodynamic calculations using thermochemical data applied in mechanism 2 showed that at the temperature range 1200 K and higher $P(OH)_3$ was the only phosphorus component. But modeling and experiment did not confirm formation of this compound in post-flame zone.

Combustion is well known to be a process controlled by radicals. Therefore, a mechanism of action all inhibitors including OPC on combustion is based on effect of inhibitor and (or) its destruction products in flame on concentarion of active flame species. Thus, a study of influence of OPC additives on profiles of temperature, concentration of stable and active (H, O, OH) species in CH_4/O_2 flames and, besides, active phosphorus-containing destruction products PO,PO_2, $HOPO$, $HOPO_2$ and $OP(OH)_3$ is the foreground task in understanding the mechanism of influence of OPC on combustion. If kinetic model of combustion of a CH_4/O_2 doped with OPC correctly predicts the concentration profiles of atoms and free radicals and phosphorus oxides and acids this model can be recognized to be perfect. Determination of concentration of H, O and OH in flames is based on partial equilibrium of three "fast" reactions. The reaction and their equilibrium constants dependence on temperature [36, 37] are given below:

$$H_2 + OH = H_2O + H \qquad \mathbf{K_1 = 0{,}113T^{0{,}0839}e^{7680/T}} \qquad \mathbf{(1)}$$

$$H_2 + O = H + OH \qquad \mathbf{K_2 = 1{,}8T^{0{,}027}e^{-917/T}} \qquad \mathbf{(2)}$$

$$O_2 + H = OH + O \qquad \mathbf{K_3 = 302T^{-0{,}374}e^{-8620/T}} \qquad \mathbf{(3)}$$

The detailed equilibrium in flames at low and moderate pressures result in formation of H, O and OH in extra-equilibrium concentrations in post-flame zone. The partial equilibrium and approximation of quasi-stationary concentrations of radicals made it possible to express their concentrations as functions of concentrations of H_2, O_2, H_2O and equilibrium constants of the reactions (1)-(3) in the flame:

$$[OH] = \sqrt{K_2 K_3 [O_2][H_2]}\,; \quad [O] = \frac{K_1 K_3 [H_2][O_2]}{[H_2O]}\,; \quad [H] = \frac{[OH][O]}{K_3 [O_2]}$$

Thus, the concentrations of H, O and OH in the lean undoped $CH_4/O_2/Ar$ flame were determined and calibration coefficients of these species relatively argon were estimated. This made it possible to obtain concentration profiles of H and OH in the lean undoped flame and flame doped with 350 ppm of TMP presented in Figs. 14 and 15. Measurement of intensities of peaks at 1 and 17 amu (H and OH, correspondingly) was carried out at ionization energy of 16.5 eV. Figures 14 and 15 demonstrate that introduction of the inhibitor results in noticeable decrease of concentrations of both species. When the inhibitor was added the concentration of H decreased for about 40 % and that of OH decreased in 2 times. The results obtained demonstrate strong decrease of concentration of the most active species in atmospheric methane flame when doped with OPC. It is noteworthy that earlier [9] it was reported about increase of OH concentration for 20 % in $H_2/O_2/Ar$ flame stabilized at low pressure when an additive of TMP was introduced. But this phenomenon was observed for low pressure hydrogen flames promoted (not inhibited) by additives of TMP. As to oxygen atom, it is impossible to measure in methane flame the intensity of peak at 16 amu corresponding only O as its ionization potential (13.618 eV) is higher than ionization potential of CH_4 (12.98 eV) [38]. In Figure 16 the intensity profiles of peak at 15 amu corresponding to CH_3 in the lean $CH_4/O_2/Ar$ flame without additive and in the same flame but doped with 350 ppm of TMP are presented. The measurement of the mass peak intensity was performed at ionization energy of 14.2 eV. The profiles presented in Fig. 16 show that the additive of TMP effects the concentration of CH_3 similarly to those of H and OH decreasing it twice. So, the data shown above indicate that effectiveness of OPC as inhibitors consists in strong influence of OPC concentration of the most active flame species.

Structure of $C_3H_8/O_2/Ar$ Flames

Figure 17 shows the simulated and measured profiles of concentration of stable species C_3H_8, O_2, H_2O and CO_2 and the profile of temperature in the lean $C_3H_8/O_2/Ar$ flame without additive. Figure 18 presents the temperature and concentration profiles obtained in experiment and by modeling for the lean $C_3H_8/O_2/Ar$ flame doped with 1200 ppm of TMP. Figures 19 and 20 present the corresponding data for the rich $C_3H_8/O_2/Ar$ flame without additive and doped with 1200 ppm of TMP. Inhibition effect of the additive results in appreciable moving of the flame front away from the burner accompanied with decreases of heat losses in to the burner as it was demonstrated for $CH_4/O_2/Ar$ flames above. Maximal temperature of undoped flames ranges 1500-1600K whereas the temperature of the doped flames ranges 1700-1800 K. The temperature rise is explained by decrease of heat losses into the burner in the doped flames due to increasing of combustion zone rather than due to effect of OPC on

thermophysical properties of the flame. A kinetic model for destruction of TMP together with Konnov mechanism of propane oxidation provides an appropriate agreement between measured and simulated profiles of concentration of stable species. Besides concentration profiles of H and OH have been determined in lean undoped flame (Fig.21). Results of modeling calculation of concentration profiles of H and OH in the lean flame also shown in Fig. 23 demonstrate an agreement with experimental data.

The measured and calculated concentration profiles of final phosphorus-containing products of TMP destruction in the lean flame – PO, PO_2, HOPO, $HOPO_2$ and $OP(OH)_3$ are shown in Fig. 22. Similar results for the rich $C_3H_8.O_2$/Ar flame are plotted in Fig. 23. Comparing the data obtained for both C_3H_8/O_2/Ar flames doped with TMP one can observe appreciable differences between composition of phosphorus-containing species in the lean and rich flames. In the lean C_3H_8/O_2/Ar flames the major final product of TMP destruction is $HOPO_2$ whereas in the rich flame apart from $HOPO_2$ such compounds as HOPO, PO_2 and $OP(OH)_3$ present in higher concentrations. The difference in the final temperature in all flames is negligible. Thus, a difference in concentration of active flame components, resulting from different composition of combustible mixtures, effects on composition of phosphorus-containing compounds in flames.

Comparing calculated and measured concentration profiles of phosphorus-containing species one can observe a satisfactory agreement between experiment and modeling for the lean C_3H_8/O_2/Ar flame doped with 1200 ppm of TMP. As to the rich flame an appreciable disagreement between simulated and measured concentration profiles is observed. Final concentrations of phosphorus-containing compounds in the lean and rich C_3H_8/O_2/Ar flames obtained by experimentally and by modeling are compared in Tables 5 and 6 correspondingly.

TABLE 5. Fraction of number of moles of a phosphorus-containing compound in total number of moles of PCS (in %) in post-flame zone of the lean flame calculated using 3 different mechanisms, equilibrium state and measured experimentally

Species	Mole fractions			Equilibrium concentrations at 1760K	Experimental results Range
	1	2	3		
PO	0.0	0.0	0.0	0.0	0 - 0.2
PO_2	15.5	1.2	29.6	3.0	3 - 15
HOPO	8.3	2.5	8.6	1.9	3.6 - 6.8
$HOPO_2$	73.0	96.0	59.4	91.3	60 -100

$PO(OH)_3$	3.2	0.3	2.4	3.8	-

The simulated concentrations tabulated above are obtained using 3 different models: our model (mechanism 1), the model of Glaude et al. [18,19] (mechanism 2) and the model of Babushok-Tsang [20,21] (mechanism 3). Besides, both tables present the equilibrium concentration of the species at final flame temperature. It should be specially pointed out that equilibrium concentrations were calculated using thermochemical data recommended by Melius [4], which is used in our kinetic mechanism and the mechanism of Babushok-Tsang [20,21].

TABLE 6. Fraction of number of moles of a phosphorus-containing compound in total number of moles of PCS (in %) in post-flame zone of the rich flame calculated using 3 different mechanisms, equilibrium state and measured experimentally

Species	Mole fractions			Equilibrium concentrations at 1700 K	Experimental results Range
	1	2	3		
PO	4.3	0.0	0.2	0.8	0 - 1.1
PO_2	6.6	4.9	14.1	4.8	2 - 11.5
HOPO	63.9	61.6	75.5	85.2	22 - 41
$HOPO_2$	23.8	32.7	9.6	8.7	34 - 63
$PO(OH)_3$	1.4	0.1	0.6	0.5	5 - 15

The application of thermochemistry developed by Glaude and others predicts all phosphorus to transform into $P(OH)_3$ that is not confirmed by modeling. The data presented in Tables 2 and 3 show that all the mechanisms provide approximately the same agreement of modeling data with experimental results for the lean flame, whereas none of the mechanisms is able to predict the concentrations of phosphorus-containing species with an appropriate accuracy. Tables 2, 3 also revealed that equilibrium concentrations of these species are not achieved in both flames. Only concentration of some species is close to equilibrium ones.

Measurements of inhibition effect of OPC on burning velocity

Study the effect of number of OPC including a number of novel substances on burning velocity of stoichiometric CH_4/air and C_3H_8/air flames have been carried out at atmospheric pressure. TMP loading dependencies of burning velocity of a stoichiometric CH_4/air flame measured experimentally and calculated using our kinetic model and 4 different mechanisms of methane oxidation (see Table 2) are presented in Fig. 24. Modeling calculations showed

CHEMKIN mechanism to provide a better agreement with experimental results. Figure 25 demonstrates TMP loading dependencies of burning velocity of a stoichiometric CH_4/air flame measured experimentally and calculated using GRI 3.0 mechanism and 3 published kinetic models for action of phosphorus-containing species on combustion. As one can see all 3 models involving phosphorus substances give very close results. Analyzing Figs. 24 and 25 one can conclude that a disagreement of modeling results with experimental data can be explained possibly by drawbacks of GRI 3.0 rather than the phosphorus-involving models. Nevertheless, a disagreement with experiment can be decreased by increasing the pre-exponential factor of reaction $H+PO_2+M=HOPO+M$ in 4 times. The modeling results obtained using mechanism 1 with modified rate constant (defined as mechanism 1.1) is presented in Fig. 25.

TMP loading dependence of normalized burning velocity of a stoichiometric C_3H_8/air flame is shown in Fig. 26. Modeling using 3 published mechanisms involving OPC destruction (Fig. 26) is in a satisfactory agreement with experiment. Comparing TMP loading dependence of burning velocity of CH_4/air and C_3H_8/air stoichiometric flames (Fig. 27) one can see that TMP loading dependence of the burning velocity does not differ drastically for both methane and propane flames. Nevertheless, an inhibition effect of TMP on CH_4/air flame is slightly stronger.

The results of measurement of burning velocity of CH_4/air flames of various equivalence ratio (in the range of measurement of φ (0.9-1.5) for the flame without additive and doped with 520 ppm of TMP (Fig. 28). Burning velocities were normalized on the maximum value of burning velocity of the undoped flame. In Fig. 28 the value $\mathbf{f}=(u_{undoped}-u_{doped})/u_{undoped}$, which presents a relative decrease of burning velocity when 520 ppm of TMP is added to the flame and characterizes effectiveness of inhibitor action on a flame. Equivalence ratio dependence of **f** passes though maximum at φ=1.1-1.2

The fluorine- and nitrogen-containing volatile (in comparison with regular phosphates and phosphonates) compounds are of advanced interest. The studied OPC and some of their properties are presented in Table 7.

Table 7. Organophosphorus compounds, which were tested as flame inhibitors.

Compound	Boiling point [^{0}C] at pressure [Torr]
$(C_2H_5O)_3PO$	215 / 760
$(CF_3CH_2O)_3PO$	73 / 8
$[(CH_3)_2N]_3PO$	123 / 19

$(CH_3O)_3PO$	180 / 760

Dependencies of inhibiting effectiveness of OPC tabulated above for propane flame are presented in Fig. 29. The data shown in Fig. 29 demonstrate that all tested OPC have approximately the same flame inhibiting effectiveness. F and N atoms introduced in molecules of some OPC do not influence on properties of OPC as flame inhibitors.

Measurement of extinction strain rate in a non-premixed CH_4/O_2 flame

The extinction strain rate in a non-premixed methane flame with OPC loading stabilized on the opposed-jet burner at 1 atmosphere was measured. The opposed-jet burner was designed in accordance with recommendations of [39]. The internal diameter of nozzles was 6.8 mm, the distance between nozzles was 6.8 mm. The flame stabilized on the fuel side of stagnation plane. The sheath flow was Ar. The maximum of flow rate was 50 cm^3/s for both fuel and oxidizer. The burner was aligned upright. Flow rates of the components are presented in Table 8.

Table .8.Volumetric flow rate (NTPcm^3/s) of the components of combustible mixture.

FUEL		OXIDIZER	
CH_4	N_2	O_2	N_2
10	40	20	30

The strain rate was calculated according to equation [40]:

$$a = \frac{2V_{ox}}{L}\left(1+\frac{V_{fuel}}{V_{ox}}\sqrt{\frac{\rho_{fuel}}{\rho_{ox}}}\right)$$

here V is the stream velocity and ρ is the stream density; L is the separation distance between nozzles. The typical value of strain rate for flames varies from 100 to 800 s^{-1} [39,41,42] and depend from the composition of fuel and oxidizer and burner design. In our experiment the value of strain rate without loading OPC was 750 s^{-1}. The extinction strain rates were measured by increasing the flow rates of fuel and oxidizer until flame is quenched. The loading of TMP ($(CH_3O)_3PO$) was from 500 to 3650 ppm and TEP ($((C_2H_5O)_3PO$) was from 500 to 1200 ppm. In Fig. 30 normalized extinction strain rate of the flame without additive and doped with of OPC are shown as a function of OPC loading. The data obtained demonstrate that TMP and TEP loading dependence of the burning velocity practically are equal for both compounds.

CONCLUSION

Sensitivity analysis of phosphorus-involving reactions of our mechanism was performed to determine the reactions, which control the burning velocity of a doped CH_4/air flame. Six reactions are specified in Fig. 31. The stage $H+PO_2+M=HOPO+M$ was demonstrated to be the most important (sensitivity coefficient -35). The rate constants of this reaction accepted by the authors of different kinetic mechanisms are tabulated below.

Table 9. Rate constant (expressed as $AT^ne^{-E/kT}$) of the reaction $H+PO_2+M=HOPO+M$ in different kinetic models

MECHANISM	***A***	n	E (kal/mol)	$A/A_{Twarowski}$
our mechanism	9.73×10^{24}	-2.0	645.0	10.0
Glaude et al. [18,19]	1.46×10^{25}	-2.0	645.0	15.0
Babushok-Tsang [20,21]	5.00×10^{24}	-2.0	645.0	5.1
Twarowski [5-7]	9.73×10^{23}	-2.0	645.0	1.0

The data presented in Table 9 indicate that pre-exponential factor of rate constant of this reaction accepted in all models except Twarowski one are very close (differ within 2.25 times). Besides the temperature dependence of the rate constants is the same in all the models. That is why the results of calculation of burning velocity using these mechanisms are very close. It means that a essentially different models but having a close rate constant of the key reactions can provide a good agreement with experiment. It is noteworthy that all authors do not accept the value of rate constant of this reaction recommended by Twarowski. Another important reactions and their rate constants recommended by different authors are tabulated below.

Table 10. The most important reactions responsible for inhibition effect and their rate constants in our model, model of Glaude et al., model of Babushok-Tsang (expressed as $k = A\,T^n*\exp(-E/RT)$)

Reaction	*our model*			*Glaude et al.*	*Babushok-Tsang*
	A		*E*	*A*	*A*
$OH+PO_2+M=HOPO_2+M$	1.6×10^{25}	-2.28	285.0	1.6×10^{24}	1.6×10^{24}
$H+HOPO_2=H_2O+PO_2$	6.32×10^{11}	0.00	11930.0	6.32×10^{12}	6.32×10^{12}
$H+PO_2+M=HOPO+M$	9.73×10^{24}	-2.04	645.0	9.73×10^{25}	9.73×10^{24}
$OH+HOPO=H_2O+PO_2$	3.16×10^{11}	0.00	0.0	3.16×10^{12}	3.16×10^{12}
$H+HOPO=H_2+PO_2$	7.9×10^{11}	0.00	43.0	7.9×10^{12}	7.9×10^{11}
$O+HOPO=OH+PO_2$	1.58×10^{12}	0.00	0.0	1.58×10^{13}	1.58×10^{13}
$O+HOPO+M=HOPO_2+M$	1.3×10^{24}	-2.11	995.0	1.3×10^{23}	1.3×10^{23}
$O+HOPO_2=O_2+HOPO$	6.32×10^{11}	0.00	8236.0	6.32×10^{12}	6.32×10^{12}

Units are mol, cm^3 , s, K and $cal\times mol^{-1}$.

Temperature dependence for all rate constants is recommended by Twarowski and the same in all 3 models. To analyze if the key stages are the same for rich and lean C_3H_8/air flames sensitivity coefficients on burning velocity were calculated (Table 11).

Table 11. The coefficients of sensitivity for burning velocity (in %) of the lean (φ=0.8) and rich (φ=1.2) C_3H_8/air flames.

N	Reaction	$\xi=(u_0-u_{k/5}/u)\times100\%$	
		φ=0.8	***φ=1.2***
1.	$H+PO_2+M=HOPO+M$	-12.7	-12.2
2.	$O+HOPO=PO_2+OH$	-4.7	-4.2
3.	$OH+PO_2+M=HOPO_2+M$	3.0	0.8
4.	$OH+HOPO=H_2O+PO_2$	-1.6	-4.9
5.	$H+HOPO_2=H_2O+PO_2$	-1.2	-3.2
6.	$O+HOPO_2=O_2+HOPO$	-1.1	2.0

Where u_0 - burning velocity at recommended rate constant; $u_{k/5}$ - burning velocity calculated with the rate constant reduced in 5 times. Table 11 shows that the sensitivity coefficients of a reaction on burning velocity may depend on equivalence ratio of a flame. Thus, reaction 4 (Table 11) is the second one on importance for the rich C_3H_8/air flame and the fourth for the lean flame.

As phosphorus-containing products of OPC destruction in a flame are known to be responsible for inhibition effect an appreciable efforts were made to measure and simulate their concentration profiles. Two other published models for OPC destruction in a flame were validated by comparing simulated and experimental profile of concentration of these products. There are several conclusions, which can be done.

None of the tested models can predict concentration profiles of PO, PO_2, HOPO, $HOPO_2$ and $OP(OH)_3$ in the rich flames. It can be connected with insufficient understanding of combustion chemistry of rich flames as well as combustion chemistry of OPC. As an illustration several examples can be cited. Possibility of presence of the species, which are the products of addition of hydrocarbon radicals to phosphorus oxides in rich flames was reported in paper [34]. A variety of PCS of complex structure was found in combustion products of rich C_2H_2/O_2/Ar flames doped with TMP and tri(dimethylamino)phosphine. Results reported in [35] indicate that combustion chemistry of OPC is not well understood. Thus, the experimental data obtained demonstrated that an additive of DMMP to the lean and rich

methane-oxygen atmospheric flame results in rise of concentration of CH_3OH in 10 times. But results of modeling using mechanisms 2 and 3 failed to describe this fact.

The models for oxidation of hydrocarbons, especially those involving C_2-C_4 species may contain rate constants, which are determined insufficiently accurate. The influence of a model for methane oxidation on final concentration of phosphorus-containing species in the lean and rich $CH_4/O_2/Ar$ flame doped with 2200 ppm of TMP can be demonstrated by the following data shown in Tables 12 and 13.

Table 12. Final concentrations of phosphorus-containing species in lean $CH_4/O_2/Ar$ flame doped with 2200 ppm of TMP calculated using our inhibition mechanism and 3 different mechanisms of CH_4 oxidation.

Species	***Experimental data***	Simulated final concentrations using our model for TMP destruction and 3 different models for CH_4 oxidation		
		CHEMKIN	Konnov	GRI 3.0
PO	0 - 0.6	0	0	0
PO_2	1 – 5	11.7	8.7	7.7
HOPO	4.8 - 8.8	4.4	3.1	2.7
$HOPO_2$	58 – 100	76.8	81.5	82.0
H_3PO_4	4.5 - 13.5	7.1	7.6	7.6

Table 13. Final concentrations of phosphorus-containing species in rich $CH_4/O_2/Ar$ flame doped with 2200 ppm of TMP calculated using our inhibition mechanism and 3 different mechanisms of CH_4 oxidation.

species	***Experimental data***	Final concentrations obtained using our model for TMP destruction and 3 models for CH_4 oxidation		
		CHEMKIN	Konnov	GRI 3.0
PO	1.9÷9.5	4.2	2.6	2.9
PO_2	2.2÷11.0	8.1	7.9	7.8
HOPO	62.6÷93.8	60.7	50.7	53.3
$HOPO_2$	6.6÷12.1	26.1	37.3	34.6
H_3PO_4	0	1.0	1.5	1.3

Although the concentrations simulated using different methane oxidation mechanisms differ not more than in 1.5-2 this fact is of interest. The modeling results can be explained by different concentrations of active species predicted by different mechanisms of methane combustion as phosphorus-containing components of a flame react actively with free atoms and radicals. As the concentration of active species in the studied flames is higher than summary concentrations of phosphorus species a small change in concentration can result in appreciable change of concentrations of phosphorus-containing products.

Table 14. Calculated maximal concentration of active species in the in the rich $CH_4/O_2/Ar$ flame doped with 2200 ppm TMP.

Species	CHEMKIN	Konnov	GRI 3.0
H	1.61×10^{-3}	9.75×10^{-4}	1.03×10^{-3}

OH	4.64×10^{-4}	3.94×10^{-4}	3.87×10^{-4}
O	8.34×10^{-5}	4.32×10^{-5}	5.45×10^{-5}

Thus, it is difficult to expect an agreement between simulated and measured concentration of phosphorus-containing species better than ±50 % for several flames simultaneously. In spite of necessity of further modification of the models describing inhibition action of OPC on a flame, the problems with a kinetic mechanism of hydrocarbon oxidation should be taken into consideration.

The ways of further work on refining of the models for inhibition of combustion should be discussed. The updating a model with new stages involving phosphorus-containing compounds seems to be a good idea. But the example of published models demonstrated that an introduction of new stages describing the interaction of phosphorus oxides with carbon-containing species was not quite helpful. The introduction of additional stages should be well-founded and directed to solution of definite problems and based on sensitivity analysis. Another way of refinement consists in calculation of rate constants of reactions. Although this way is very difficult and consumes a lot of time it seems to be on of prospective.

REFERENCES

1. Korobeinichev, O.P., Chernov, A.A., Shvartsberg, V.M., *Preprint Pap. Am. Chem. Soc., Division of Fuel Chemistry* 39: 193 (1994).
2. Korobeinichev O.P., Ilyin S.B., Mokrushin V.V., Shmakov A.G., *Combust. Science and Technology* 116-117: 51 (1996).
3. Werner, J.H., and Cool, T.A., *Combust. Flame* 117: 78 (1999).
4. Melius, C., http://herzberg.ca.sandia.gov/carl_melius.html/
5. Twarowski, A..J., *Combust. Flame* 94: 91 (1993).
6. Twarowski, A.J., *Combust. Flame* 102: 55 (1995).
7. Twarowski, A.J., *Combust. Flame* 105: 407 (1996).
8. Korobeinichev, O.P., Ilyin, S.B., Shvartsberg, V.M., and Chernov, A.A., *Combust. Flame* 118: 718 (1999).
9. Korobeinichev, O.P., Shvartsberg, V.M., and Chernov, A.A., *Combust. Flame* 118: 727 (1999).
10. Korobeinichev, O.P., Ilyin, S.B, Bolshova, T.A., Shvartsberg, V.M., Chernov, A.A., *Combust. Flame* 121: 593 (2000).
11. Korobeinichev, O.P., Chernov, A.A., Bolshova, T.A. *Combust. Flame* 123: 412 (2000).

12. Korobeinichev, O.P., Bolshova, T.A., Shvartsberg, V.M., Chernov, A.A. *Combust. Flame* 125: 744 (2001).
13. Korobeinichev, O.P., Bolshova, T.A., Shvartsberg, V.M., Chernov, A.A., and Mokrushin, V.V., *Proceedings of Halon Option Technical Working Conference*, Albuquerque, NM, 1999, p.488.
14. Korobeinichev, O.P., Mamaev, A.L., Sokolov, V.V., Bolshova, T.A., and Shvartsberg V.M., *Proceedings of Halon Options Technical Working Conference*, Albuquerque, NM, 2000, p.164.
15. Korobeinichev, O.P., Mamaev, A.L., Sokolov, V.V., Bolshova, T.A., Shvartsberg, V.M., *Proceedings of Halon Option Technical Working Conference*, Albuquerque, NM, 2001, p.173.
16. MacDonald, M.A., Gouldin, F.C., Fisher, E.M. *Combust. Flame* 124:668 (2001).
17. Kaizeman, J.A., Tapscott, R.E., "*Advanced Streaming Agent Development. Vol. 3. Phosphorus Compounds*", NMERI, Report No. NMERI 96/5/32540, 1996.
18. Glaude P.A., Curran H.J., Pitz W.J. and Westbrook C.K., "Kinetic Study of the Combustion of Organophosphorus Compounds", *Proceedings Twenty-Eighth Symposium (International) on Combustion*, The Combustion Institute, Pittsburgh, 2001, vol. 28, page 1749
19. http://www-cms.llnl.gov/combustion/combustion_home.html.
20. Wainner, R.T., McNessby, K.L., Daniel, R.G., Miziolek, A.W., Babushok, V.I., *Proceedings of Halon Option Technical Working Conference*, Albuquerque, 2000, p.141.
21. Babushok, V., Tsang, W., *Proceedings of the Third International Conference on Fire Research and Engineering*, Society of Fire Protection Engineers, Bethesda, 1999, p.257.
22. Korobeinichev, O.P., Tereshenko, A.G., Emel'yanov, I.D., Fedorov, S.Y., Kuibida, L.V., and Lotov V.V., *Combust. Explos. Shock Waves* 21: 524 (1985).
23. Bastin, E., Delfau,J.-L., Reuillon, M., Vovelle, C., Warnatz, J., *Proceedings Twenty-Second Symposium (International) on Combustion*, The Combustion Institute, Pittsburgh, 1988, p.313.
24. Vandooren, J., and Bian, J., *Proceedings Twenty -Third Symposium (International) on Combustion*, The Combustion Institute, The Combustion Institute, Pittsburgh, 1990, p.839.
25. Korobeinichev, O.P., Shvartsberg, V.M., Ilyin, S.B., Chernov, A.A Bolshova, T.A *Combust. Expl. Shock Waves,* 3, 1999.

26. Fristrom, R.M., *Flame Structure and Processes*, Oxford University Press: New York, 1995, p.124.
27. Dodonov, A.F., Karpov, S.S., Pevsner, A.S. Informational measuring system to study charged particles flows. Author certificate (Russia) 14577167. Published on 09.10.88.
28. Aparina, E.V., Balakay, A.A., Kir'yakov, N.V., Markin, M.I., and Tal'rose, V.L., *Dokl. Akad. Nauk SSSR* 262:630 (1982) (in Russian)
29. Linteris, G.T., Truett, G.T. *Combust. Flame* 105: 15 (1996).
30. Kee, R.J., Grcar, J.F., Smooke, M.D., and Miller J.A., "PREMIX", Sandia National Laboratories Report No. SAND85-8240.
31. Kee, R.J., Rupley, F.M., Miller, J.A., "CHEMKIN-II: A Fortran Chemical Kinetics Package for the Analysis of Gas Phase Chemical Kinetics," Sandia National Laboratories SAND89-8009B.
32. http://www.me.berkeley.edu/gri_mech
33. http://www.chem.leeds.ac.uk/Combustion/Combustion.html
34. Konnov, A., http://homepages.vub.ac.be/~akonnov/
35. Korobeinichev O.P., Shvartsberg V.M., Chernov A.A., Mokrushin V.V "Hydrogen Oxygen Flame Doped with Trimethyl Phosphate, Its Structure and Trimethyl Phosphate Destruction Chemistry".- In: Twenty-Sixth Symposium (International) on Combustion, Pittsburgh, PA: The Combustion Institute. 1997. P. 1035-1042.
36. Korobeinichev, O.P., Shvartsberg, V.M., Ilyin, S.B., Chernov, A.A Bolshova, T.A., *Combust. Expl. Shock Waves,* 3:239 (1999).
37. Handbook of Physical Values, (Editor - E.Z. Meilikhova). Energoatomizdat, Moscow, 1991, p.420 (in Russian).
38. Baulch, D.L., Cobos, S.J.,Cox, R.A., Esser C., Frank, P.,Just, Th., Kerr, J.A., Pilling, M.J., Troe, J., Walker, R.W., Warnatz, J. J. *Phys. Chem. Ref. Data* 21: 411-750 (1992).
39. MacDonald, M.A., Jayaweera, T.M., Fisher, E.M., and Gouldin, F.C., Proc. Combust. Inst. 27:2749 (1998)
40. Seshadri, K., Williams, F.A., Int. J. Heat Mass Transfer 21:251-253(1978)
41. Rumminger, M.D., Linteris, G.T., Combustion and Flame, 128:145-164 (2002)
42. Otsuka, Y., Niioka, T., Combustion and Flame, 21:163-176 (1973)
43. Hebgen, P., Homan, K.H., "Phosphorus Compounds as Flame Inhibitors - Analysis of Ionic Intermediates," *Proceedings Twenty-Seventh Symposium (International) on Combustion*, Pittsburgh, 1998*, Book of Abstracts,* p.497.

44. Nogueira, M.F.M., Fisher, E.M. "Effect of Dimethyl Methylphosphonate on Premixed CH_4/O_2/Ar Flame," *Proceedings of the Joint US section meeting*, The Combustion Institute, Washington, DC, March 1999.

SUMMARY OF THE MOST IMPORTANT RESULTS

- Methodic difficulties of MBMS measurement of the structure of atmospheric flames were analyzed and recommendations were elaborated. The method of evaluation of perturbation of an atmospheric flame caused by a sonic probe was proposed.
- Profiles of temperature and concentration of following species in the lean (φ=0.8) and rich (φ=1.2) $CH_4/O_2/Ar$ and $C_3H_8/O_2/Ar$ flames were measured: CH_4, C_3H_8, O_2, H_2O, CO, CO_2, H, OH, TMP, PO, PO_2, HOPO, $HOPO_2$ and $OP(OH)_3$.
- TMP loading dependence of burning velocity of stoichiometric CH_4/air and C_3H_8/air flames were measured using Mache-Hebra nozzle burner and the total area method of a flame image.
- TMP and triethylphosphate loading dependence of normalized extinction strain rate of opposed-jet $CH_4/O_2/N_2$ flame was measured. Both OPC demonstrated close fire suppression effectiveness.
- The structure of the lean (φ=0.8) and rich (φ=1.2) $CH_4/O_2/Ar$ and $C_3H_8/O_2/Ar$ flames without additives and doped with TMP and burning velocity of methane-air and propane-air flames at various concentration of TMP additives were simulated using PREMIX and CHEMKIN codes.
- Earlier proposed kinetic mechanism for TMP destruction in low pressure $H_2/O_2/Ar$ and $CH_4/O_2/Ar$ flames was refined basing on comparison of measured and calculated results on the structure and burning velocity of atmospheric flames.
- Two published models for destruction of OPC in a flame proposed by Glaude et al. and Babushok and Tsang were used for simulation of the structure and burning velocity of the flames.
- The sensitivity analysis was applied to specify the stages responsible for inhibition and their rate constants accepted for all 3 models have been compared.
- The mechanisms for methane combustion available in literature were used for simulation of concentration profiles of phosphorus-containing species and burning

velocity of a stoichiometric CH_4/air flame. Their influence on composition of phosphorus-containing flame products was demonstrated.

- Recommendations for further investigation of combustion chemistry of OPC and refinement of the kinetic model for OPC destruction in flame have been proposed.

APPENDIX

Figures

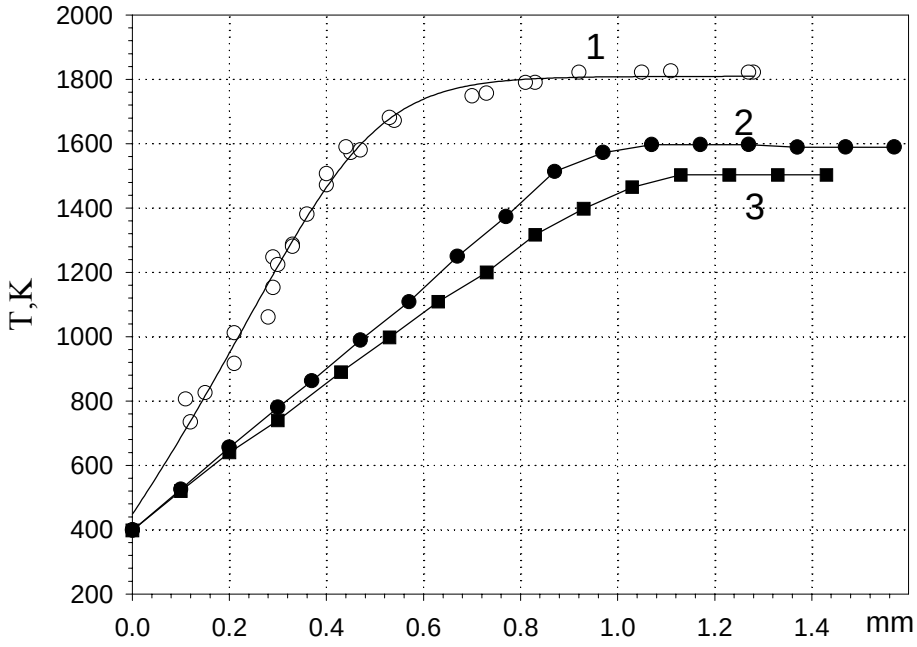

Fig.1. Temperature profiles in lean $CH_4/O_2/Ar$ (0.06/0.15/0.79) flame at 1 bar. Curve 1-without probe($\delta=\infty$), curve 2-δ=0.3mm, curve 3-δ=0.13mm.

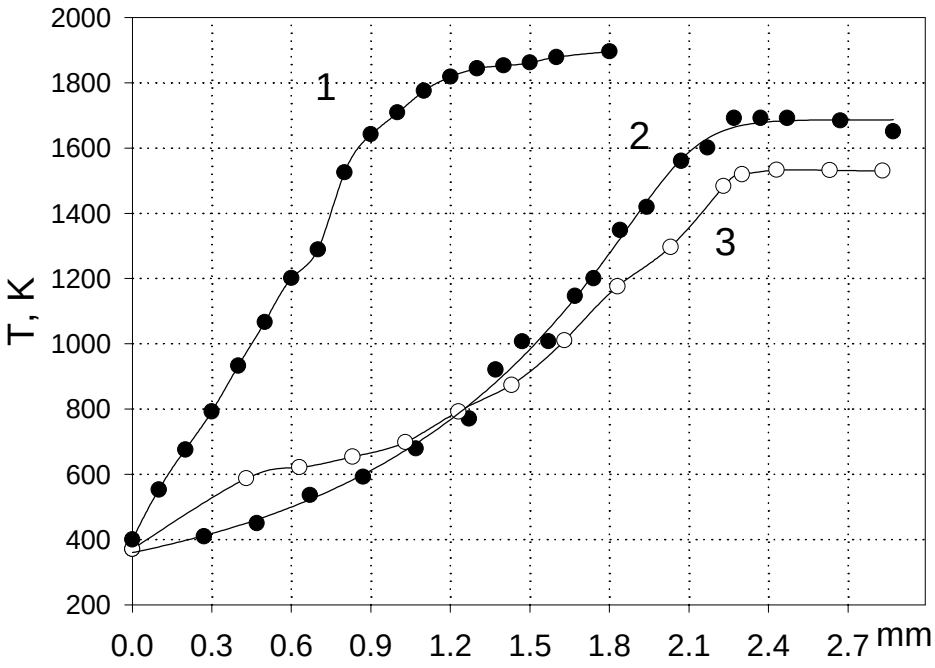

Fig.2. Temperature profiles in lean flame $CH_4/O_2/Ar$ (0.06/0.15/0.79) doped with 2200ppm of TMP at 1 bar. Curve 1-without probe ($\delta=\infty$), curve 2-δ=0.25mm, curve 3-Δl=0.1mm.

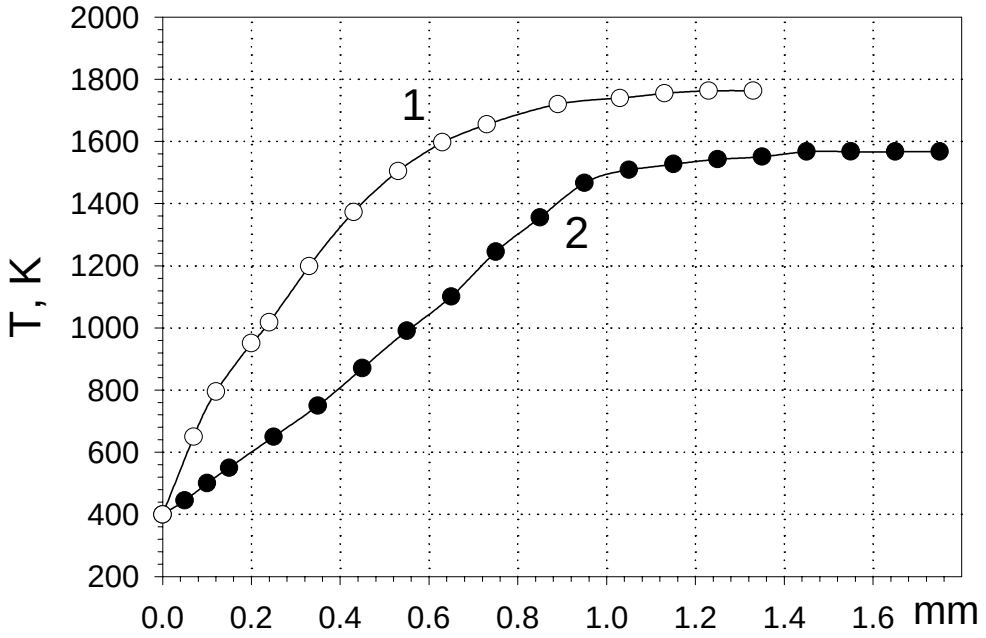

Fig.3. Temperature profiles in rich flame $CH_4/O_2/Ar$ (0.075/0.125/0.8) at 1 bar. Curve 1-without probe(δ=∞), curve 2-δ=0.3mm.

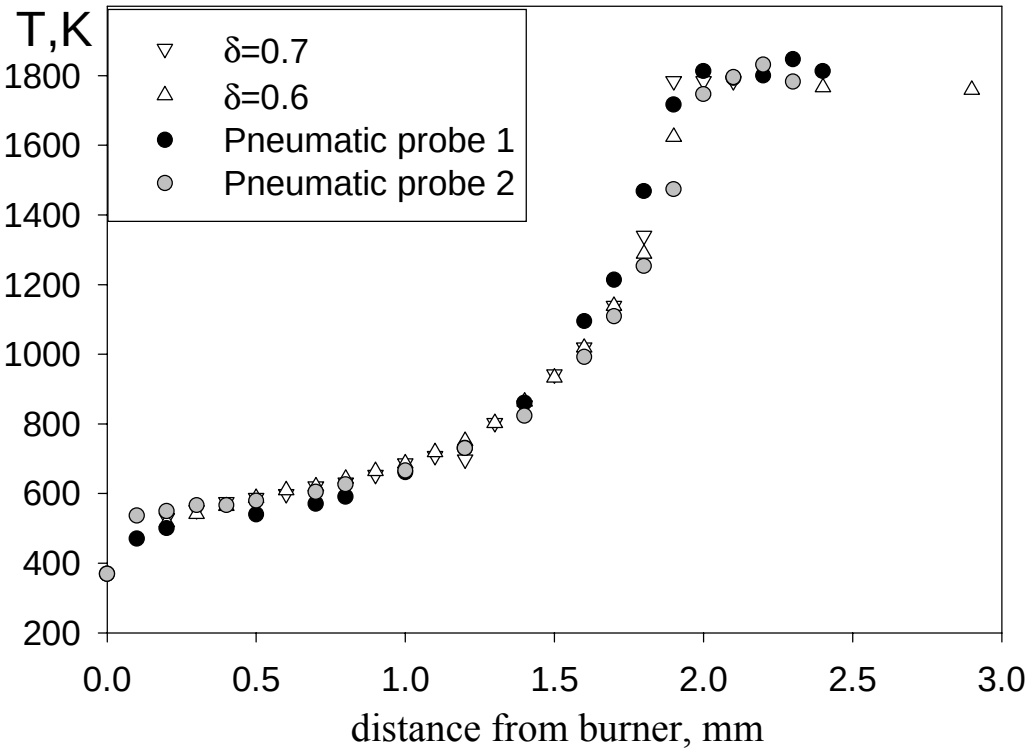

Fig. 4. Temperature profiles in the lean $CH_4/O_2/Ar$ flame doped with 1200 ppm of TMP measured by a thermocouple placed at distances δ=0.6 and 0.7 mm from the probes and by pneumatic probes.

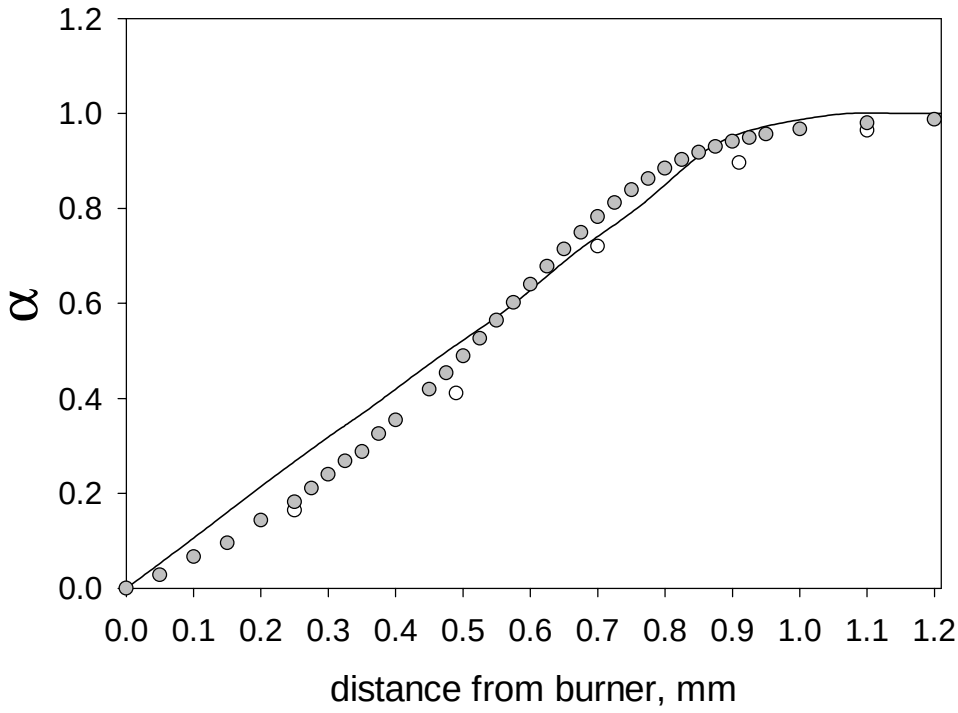

Fig. 5. Normalized profiles of temperature $\alpha_T=(T-T_0)/(T_f-T_0)$ and concentration of O_2 $\alpha_C=(C-C_0)/(C_f-C_0)$ in a near stoichiometric $CH_4/O_2/Ar$ flame without additive of TMP. Line - temperature; filled symbols - results of modeling; open symbols - results of experiment.

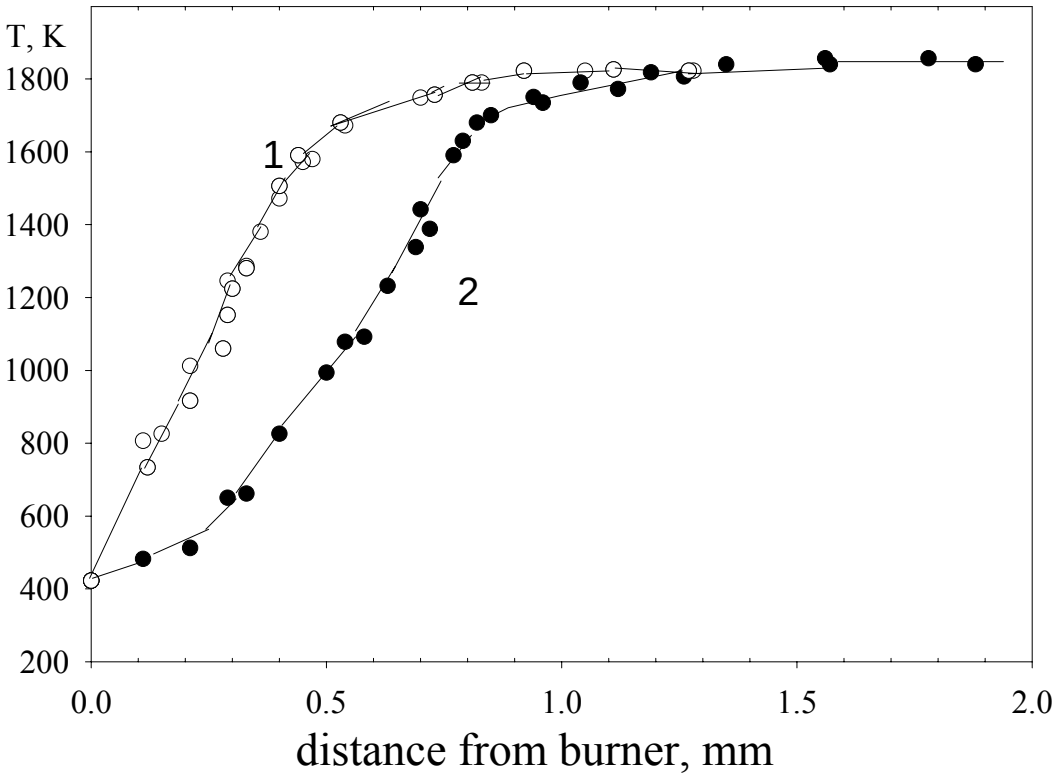

Fig. 6. Temperature profiles in the lean unperturbed $CH_4/O_2/Ar$ flame without additive (open symbols) and doped with 350 ppm of TMP (filled symbols).

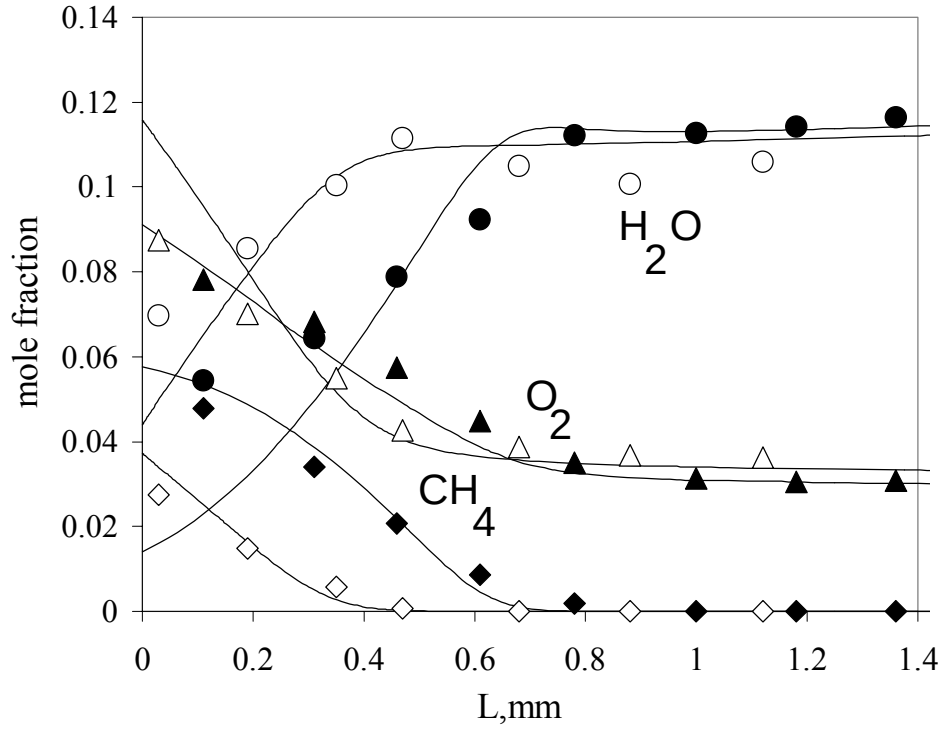

Fig. 7. Concentration profiles of CH_4, O_2, and H_2O in the lean CH4/O2/Ar flame without additive (open symbols) and doped with 350 ppm of TMP (filled symbols) obtained by microprobe technique; lines - modeling.

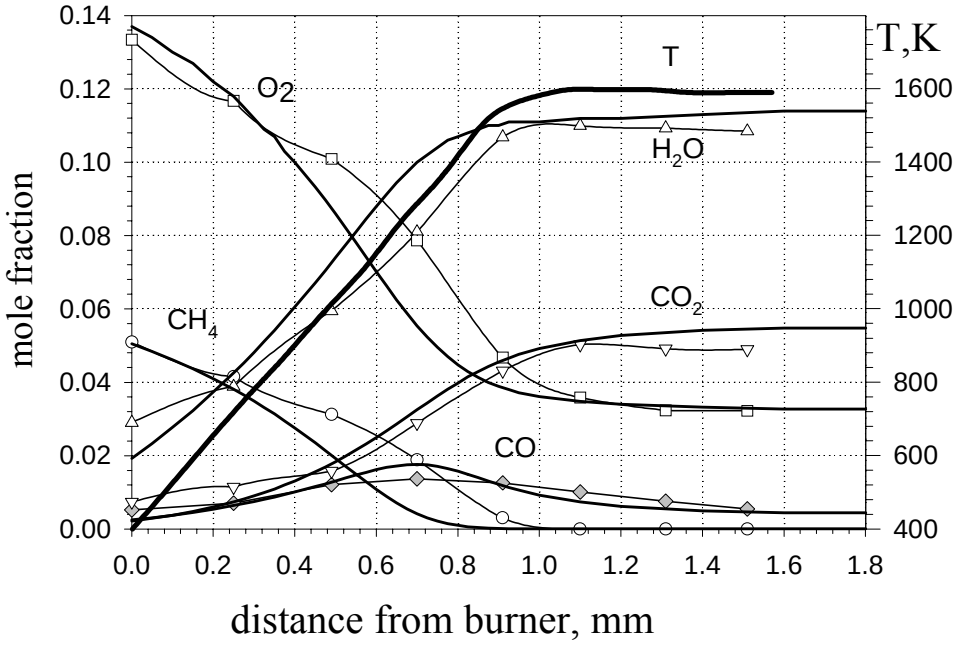

Fig.8 The concentration profiles for undoped lean $CH_4/O_2/Ar$ (0.06/0.15/0.79) flame. Solid lines – modeling; symbols – experiment (MBMS technique).

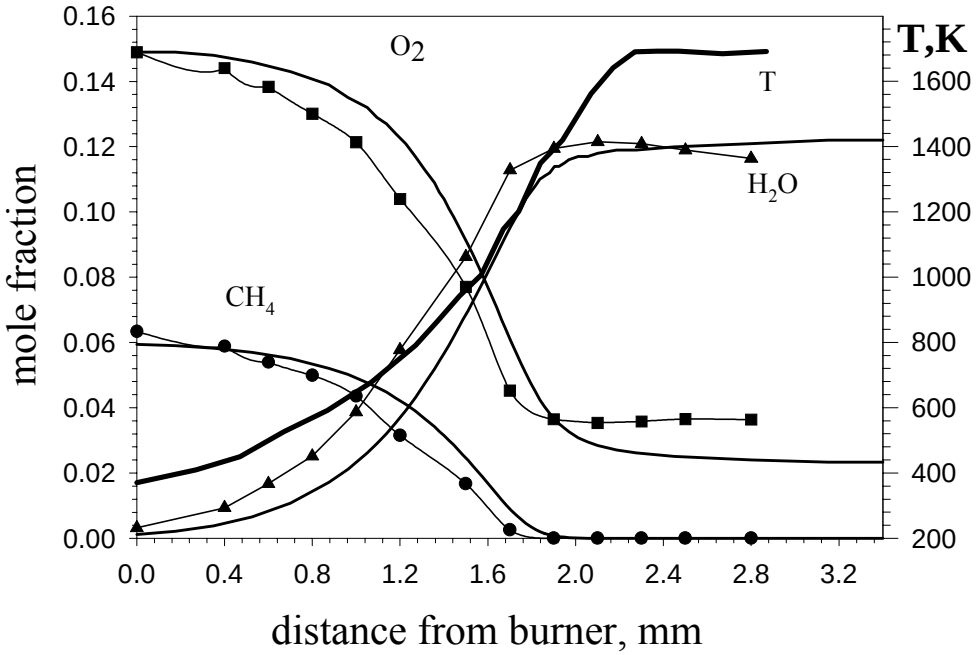

Fig.9 The concentration profiles for doped lean $CH_4/O_2/Ar$ (0.06/0.15/0.79) flame with 2200 ppm of TMP. Solid lines – modeling; symbols – experiment.

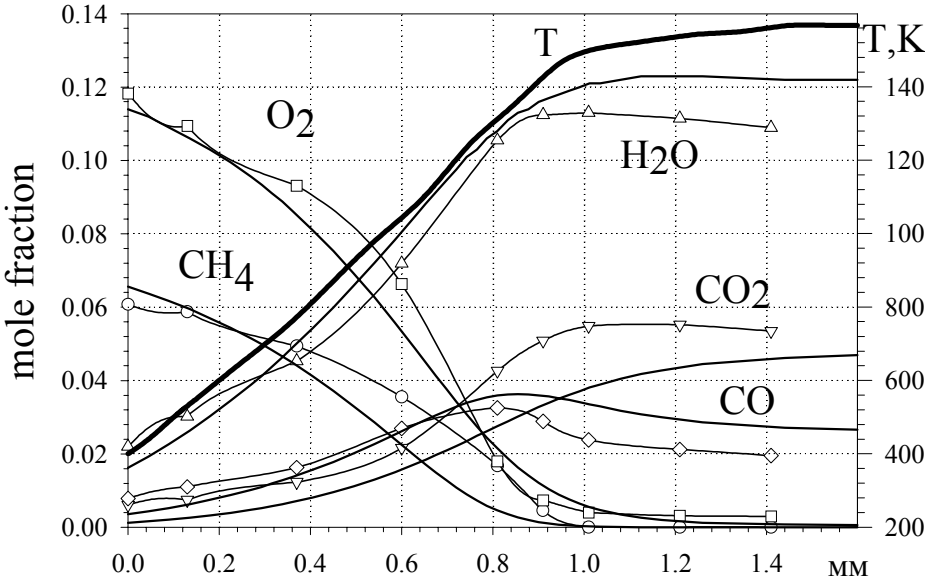

Fig. 10 The concentration profiles for undoped rich $CH_4/O_2/Ar$ (0.075/0.125/0.80) flame. Solid lines – modeling; symbols – experiment.

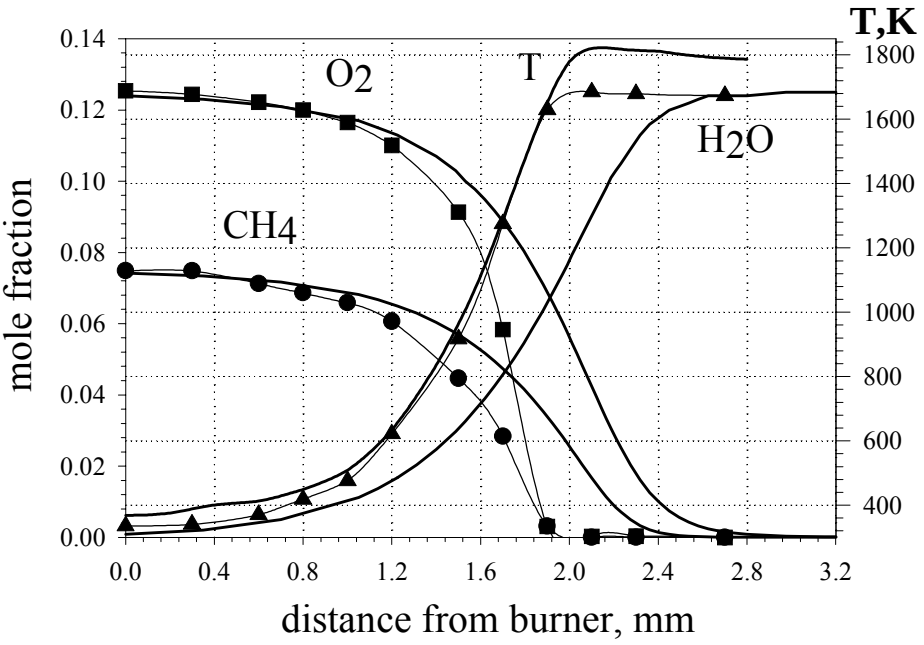

Fig. 11. The concentration profiles for doped rich $CH_4/O_2/Ar$ (0.075/0.125/0.80) flame doped with 2200 ppm of TMP. Solid lines – modeling; symbols – experiment (MBMS technique).

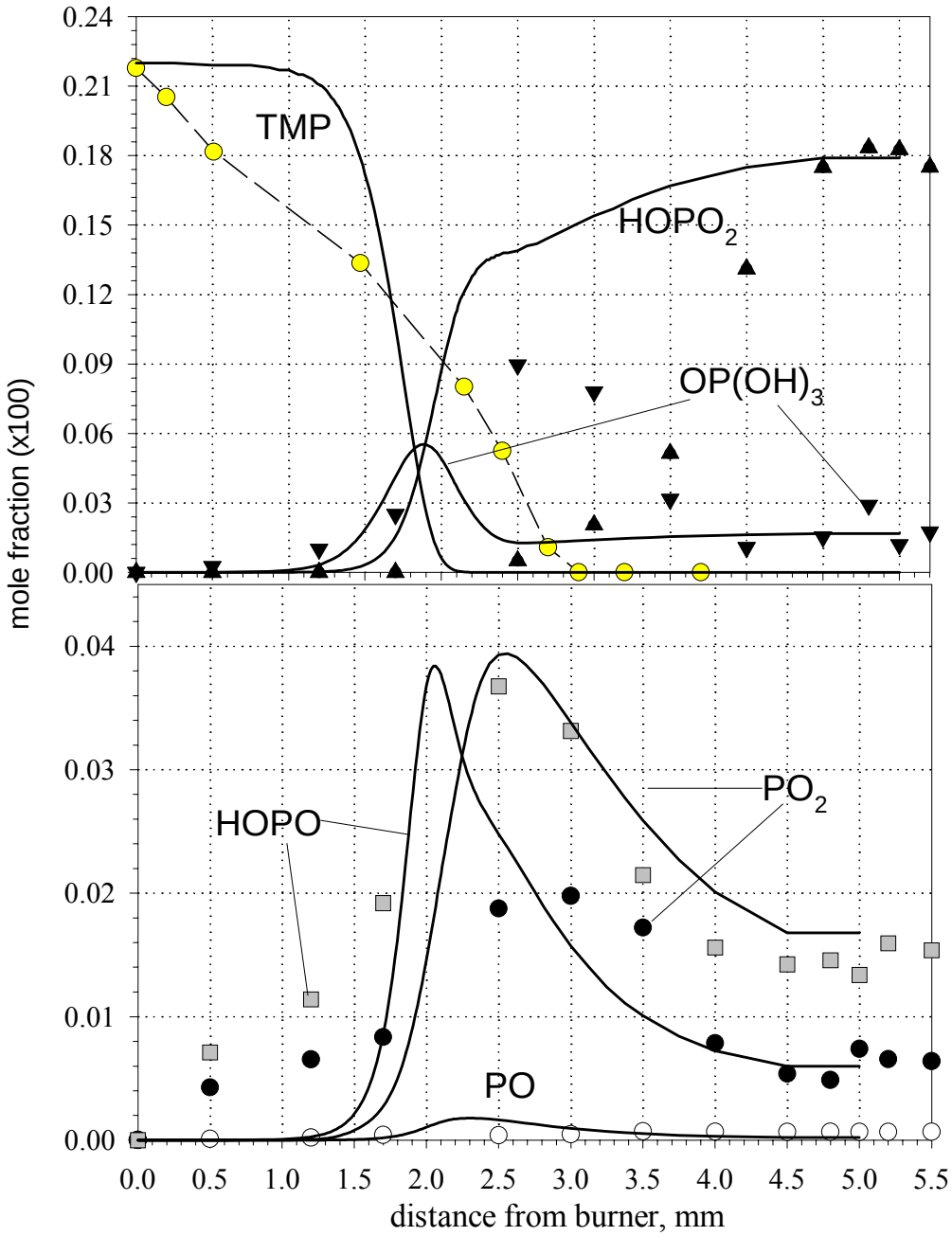

Fig. 12. Profiles of Concentration of TMP and phosphorus-containing products of its destruction in the lean $CH_4/O_2/Ar$ flame doped with 2200 ppm of TMP; symbols - experiment, lines- modeling.

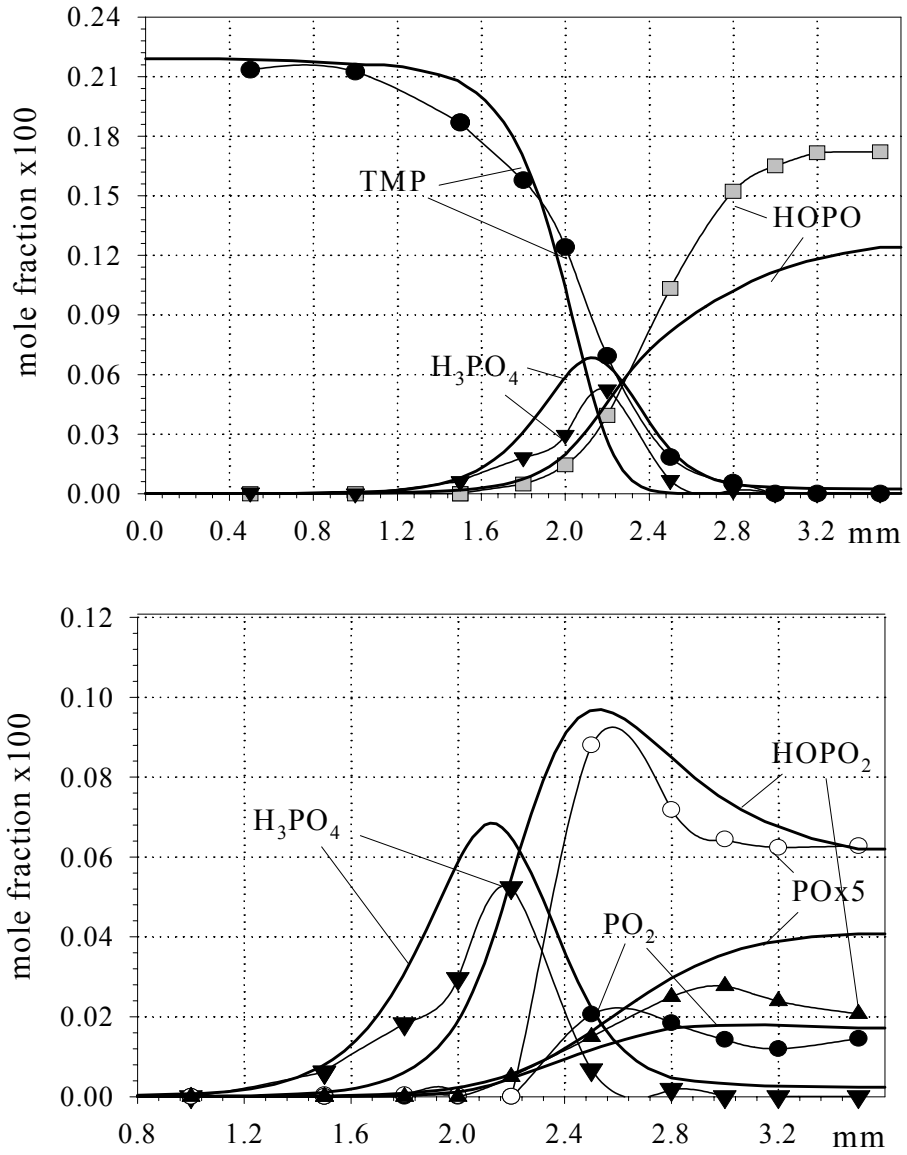

Fig. 13 Concentration profiles of TMP and phosphorus containing products of its destruction in the rich $CH_4/O_2/Ar$ (0.075/0.125/0.80) and sum of experimentally measured concentration of TMP, H_3PO_4, $HOPO_2$, HOPO, PO_2, PO. Solid lines – modeling; symbols – experiment.

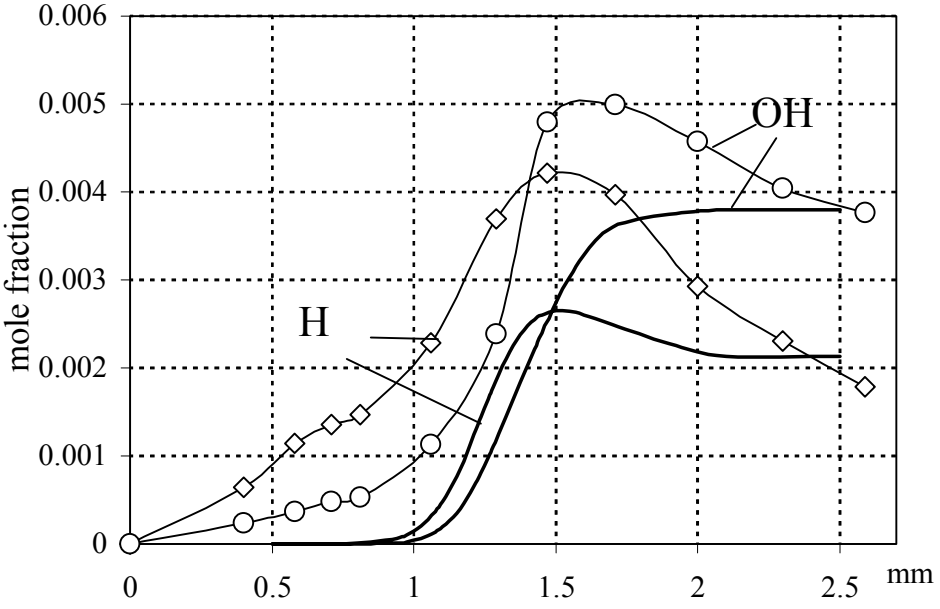

Fig. 14. Concentration profiles of H and OH in the lean $CH_4/O_2/Ar$ flame without additive.

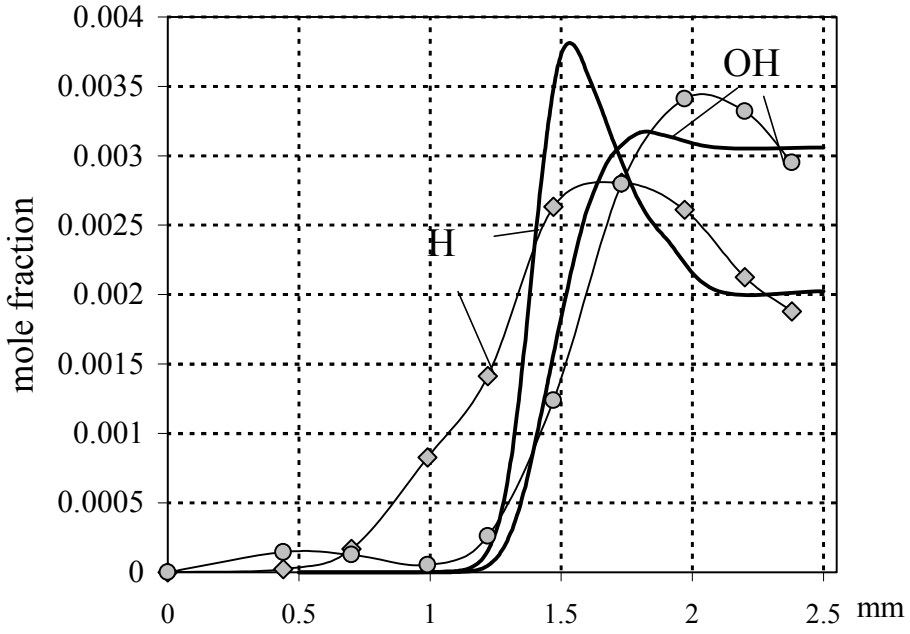

Fig. 15. Concentration profiles of H and OH in the lean $CH_4/O_2/Ar$ (0.06/0.15/0.79) flame doped with 350 ppm of TMP. Solid lines - modeling; symbols - experiment.

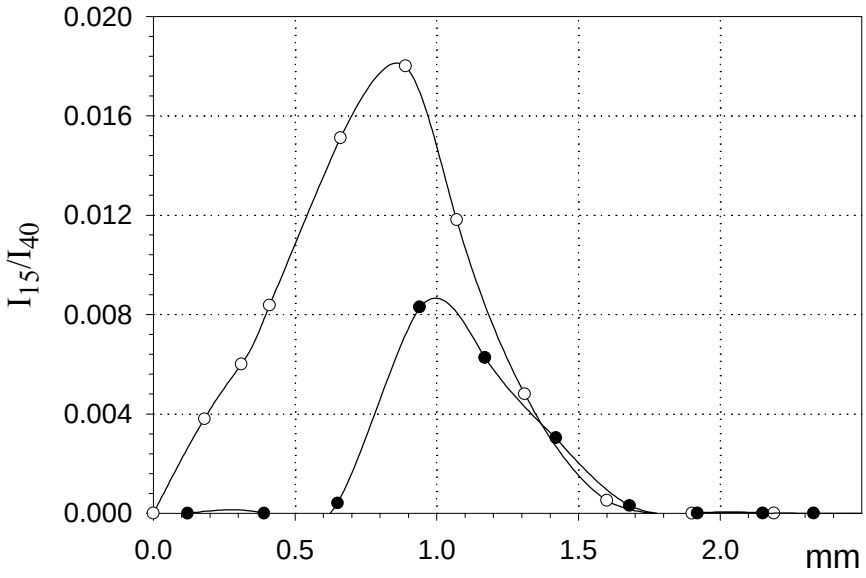

Fig. 16. Profiles of intensities of peak at 15 amu (CH_3) in the lean $CH_4/O_2/Ar$ (0.06/0.15/0.79) flame without additive (open symbols) and doped with 350 ppm of TMP (filled symbols).

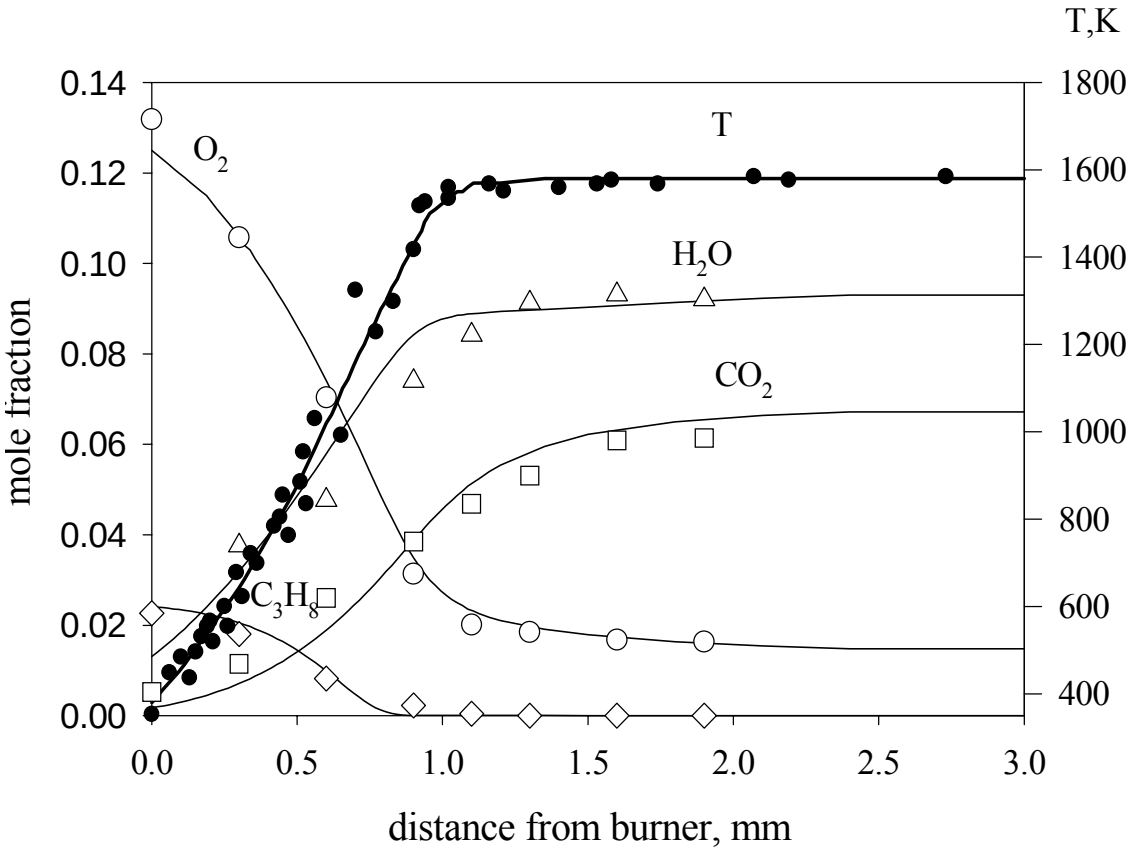

Fig. 17 Profiles of temperature (experiment) and concentration of stable species in the lean $C_3H_8/O_2/Ar$ flame without additive. Symbols - experiment, lines - modeling.

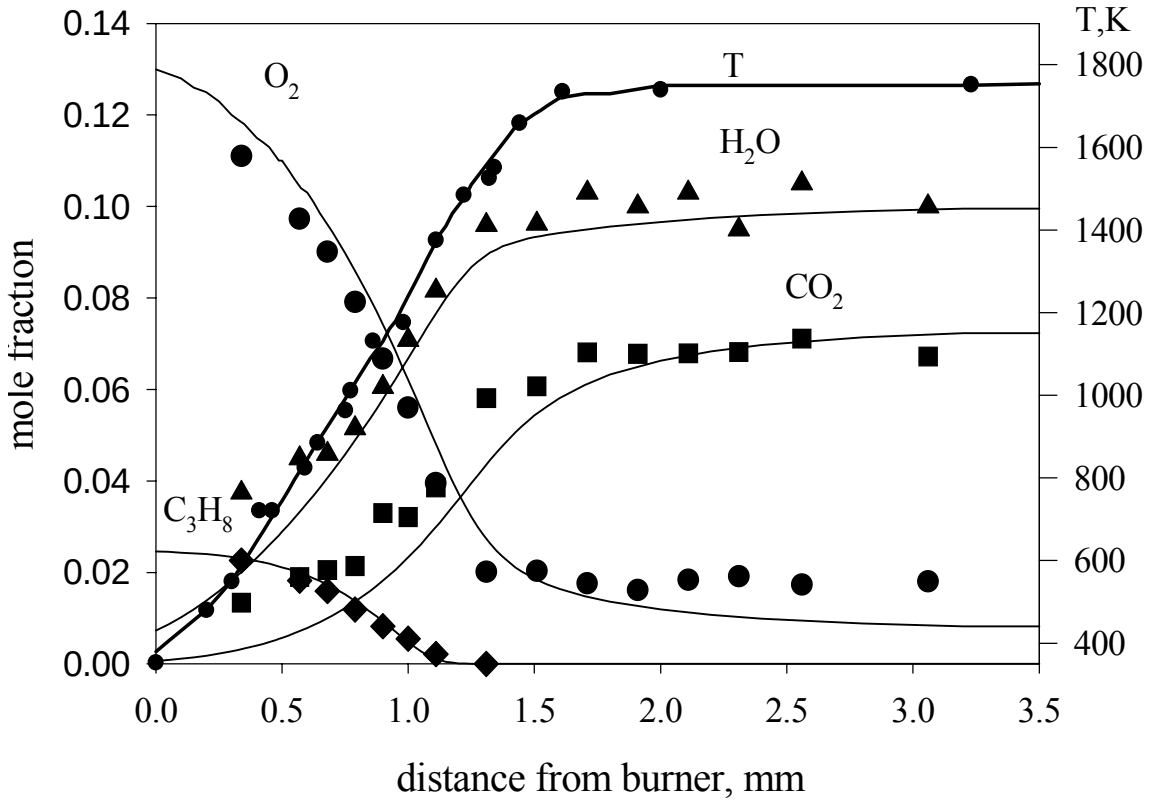

Fig. 18 Profiles of temperature (experiment) and concentration of stable species in the lean $C_3H_8/O_2/Ar$ flame doped with 1200 ppm of TMP. Symbols - experiment, lines - modeling.

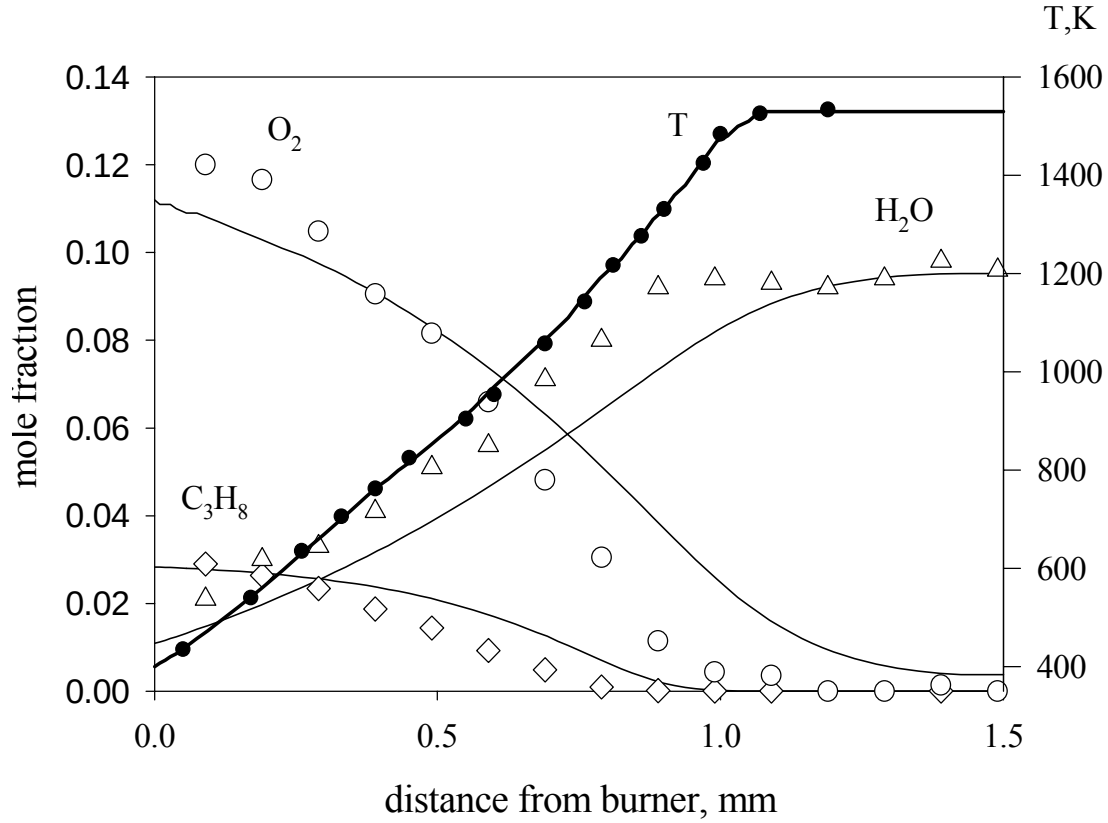

Fig. 19 Profiles of temperature (experiment) and concentration of stable species in the rich $C_3H_8/O_2/Ar$ flame without additive. Symbols - experiment, lines - modeling.

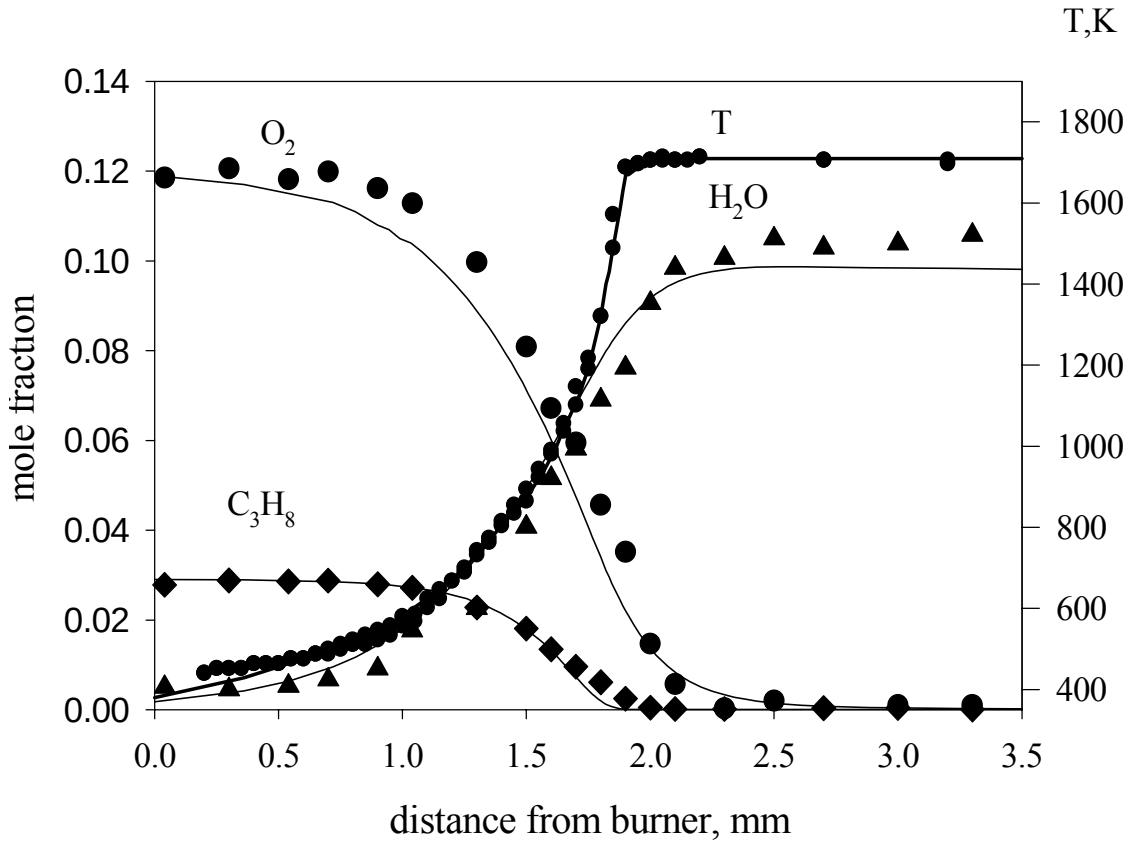

Fig. 20. Profiles of temperature (experiment) and concentration of stable species in the rich $C_3H_8/O_2/Ar$ flame doped with 1200 ppm of TMP. Symbols - experiment, lines - modeling.

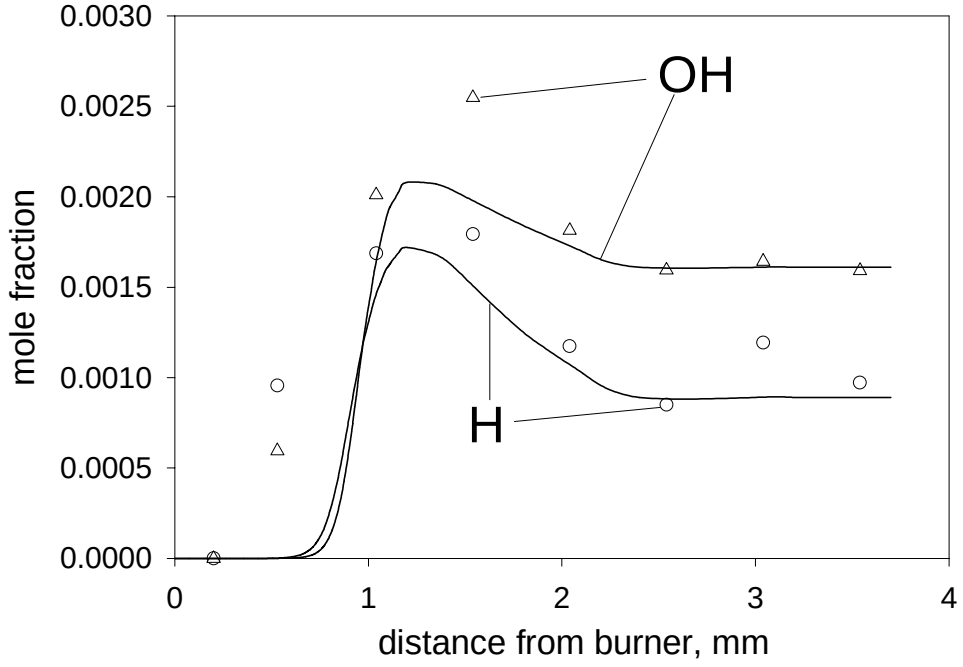

Fig. 21. Concentration profiles of H atoms and OH radicals in the lean $C_3H_8/O_2/Ar$ flame without additive. Symbols - experiment, lines - modeling.

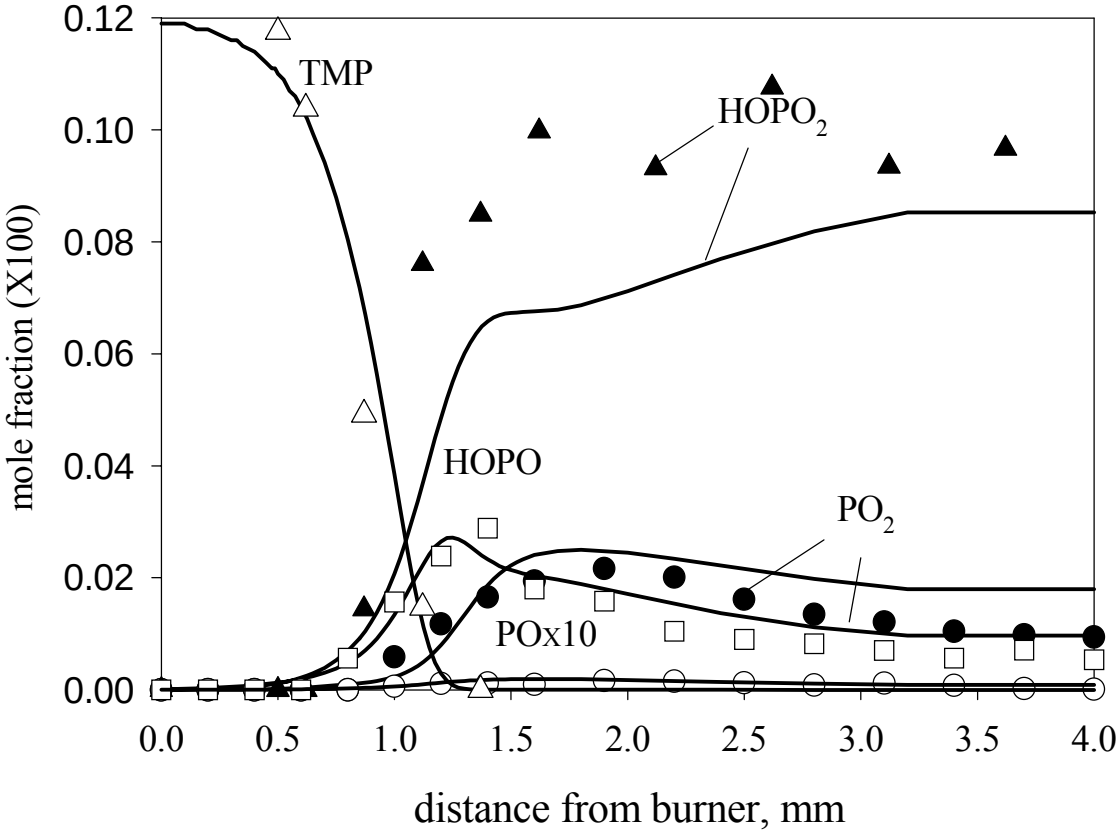

Fig. 22. Concentration profiles of TMP and of final phosphorus-containing products of its destruction PO, PO_2, HOPO, $HOPO_2$ in the lean $C_3H_8/O_2/Ar$ flame

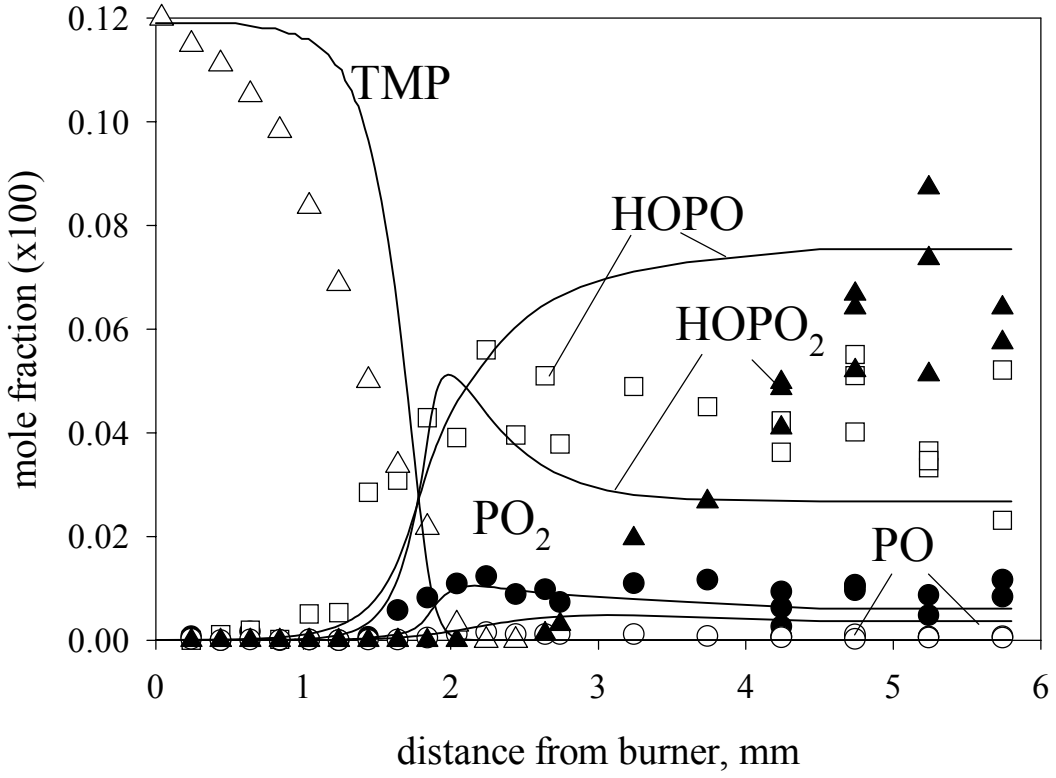

Fig. 23. Concentration profiles of final phosphorus-containing products of TMP destruction and TMP in the rich $C_3H_8/O_2/Ar$ (2.92/12.08/85) flame doped with 1200 ppm of TMP. P=1 bar. Solid lines – modeling; symbols – experiment.

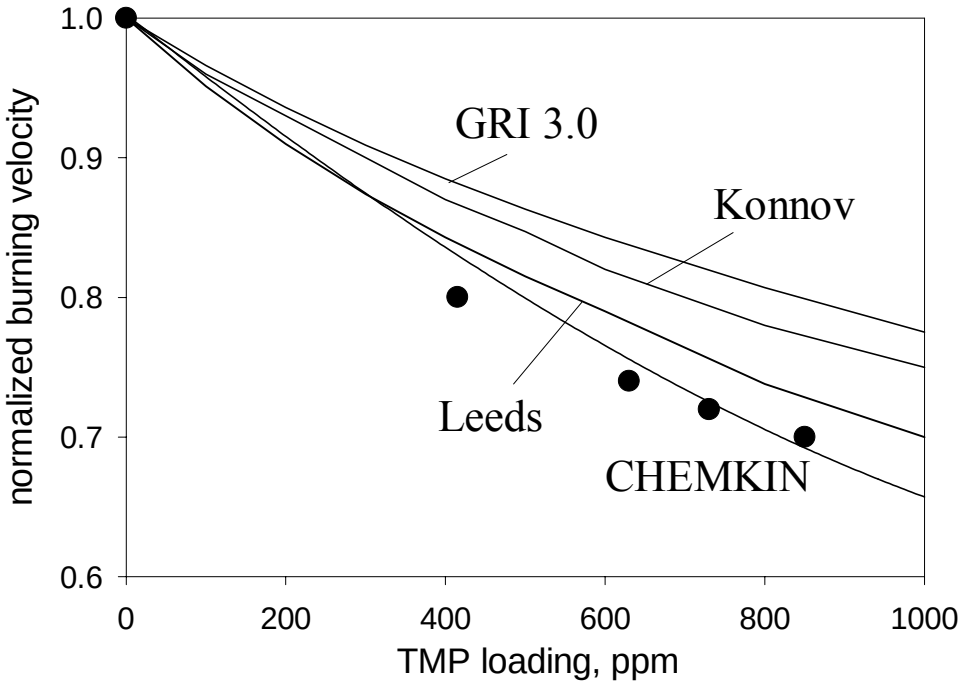

Fig. 24. TMP loading dependence of burning velocity of CH_4/air flame measured experimentally (symbols) and calculated by modeling (lines) using our TMP destruction model and 4 various models of CH_4 oxidation.

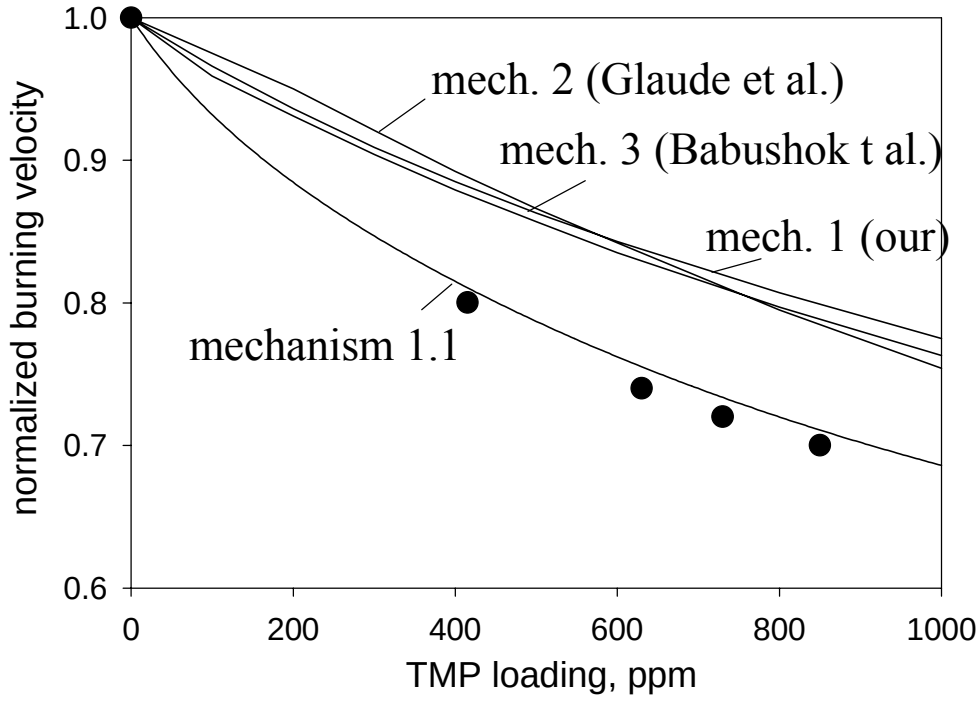

Fig. 25. TMP loading dependence of burning velocity of a stoichiometric CH_4/air. Symbols - experiment; lines - modeling performed using GRI 3.0 mechanism and mechanisms 1,2, 3 and mechanism 1.1 with modified rate constant $H+PO_2+M=HOPO+M$, $A=4.0\times10^{25}$.

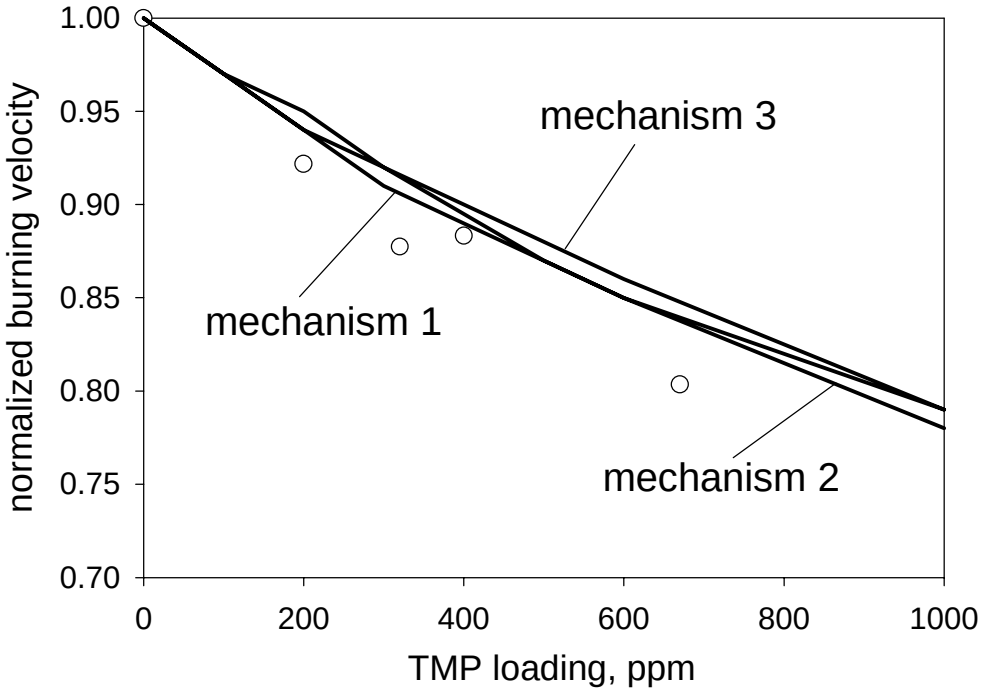

Fig. 26. Burning velocity of the stoichiometric C_3H_8 + air mixture as a function of TMP loading. Symbols - experiment; lines - modeling results obtained using three different mechanisms for C_3H_8 + air mixture.

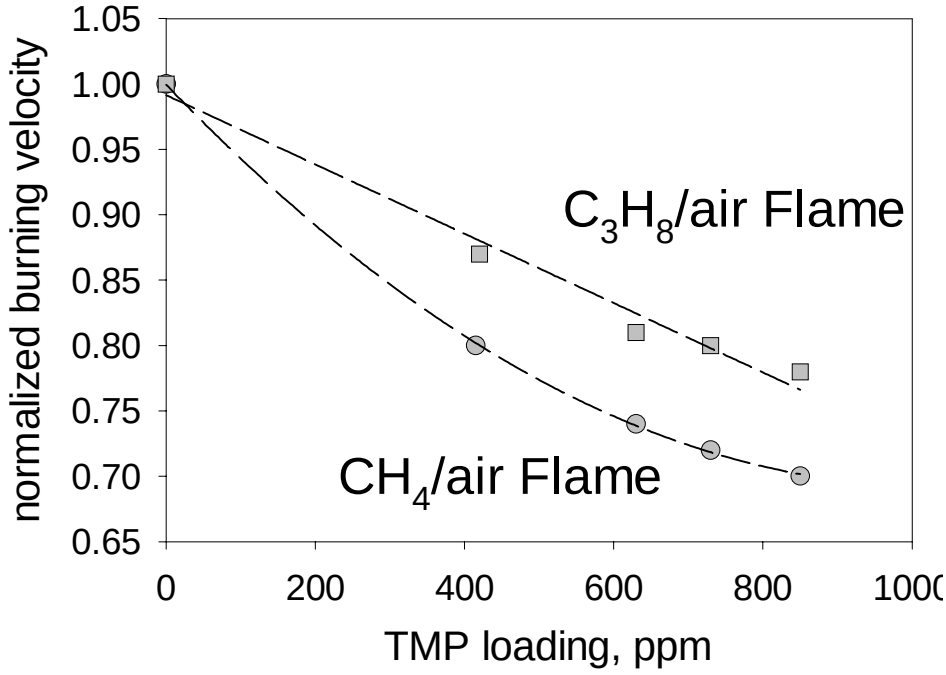

Fig. 27. TMP loading dependence of burning velocity of CH_4/air (circle) and C_3H_8/air (square) flames (experiment).

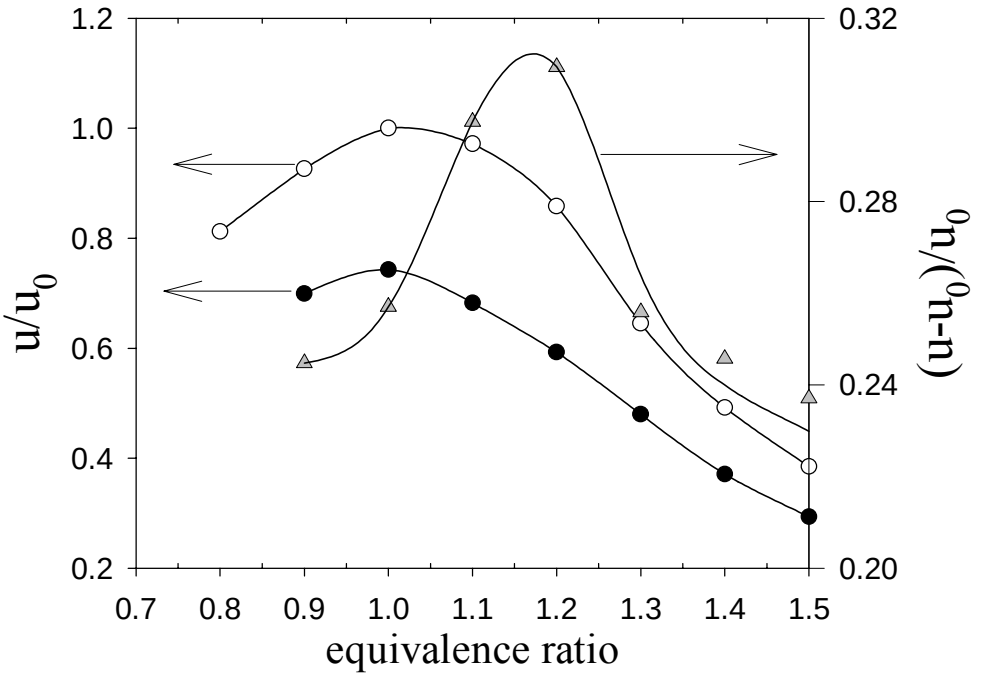

Fig. 28. Equivalence ratio dependence of burning velocity of CH_4/air flames without additive and doped with 520 ppm of TMP.

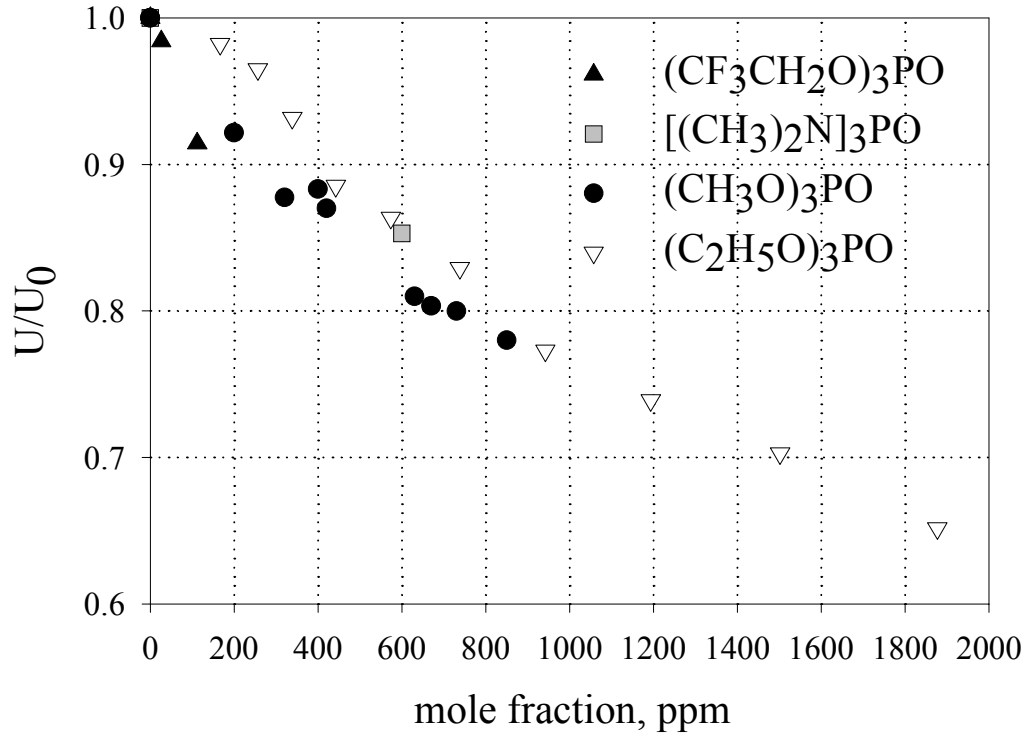

Fig. 29 Normalized burning velocity of stoichiometric C_3H_8 – Air flame as a function inhibitor loading.

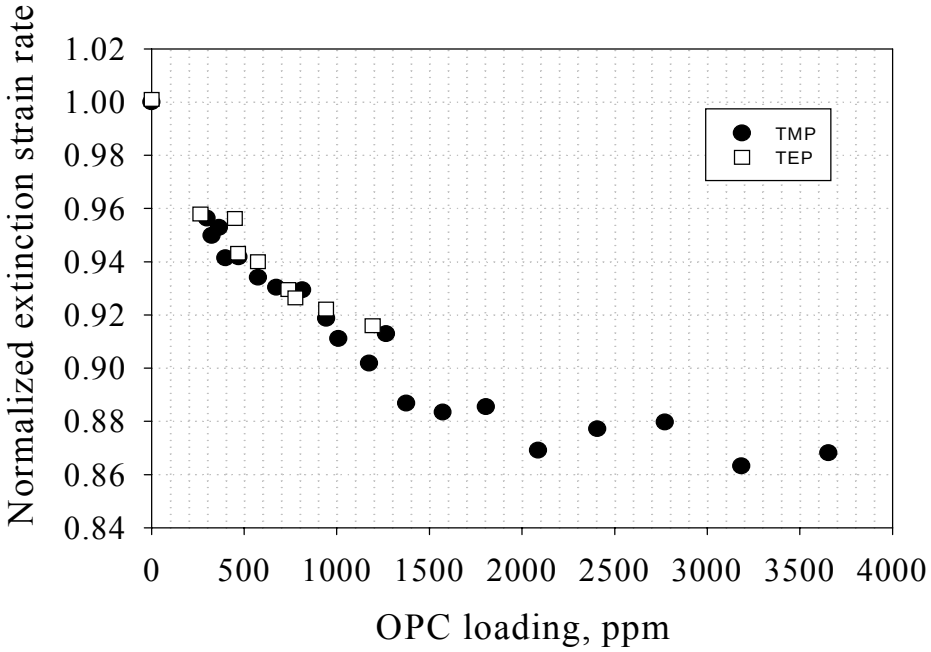

Fig.30 Normalized extinction strain rate of the flame without additive and doped with of OPC as a function of OPC loading.

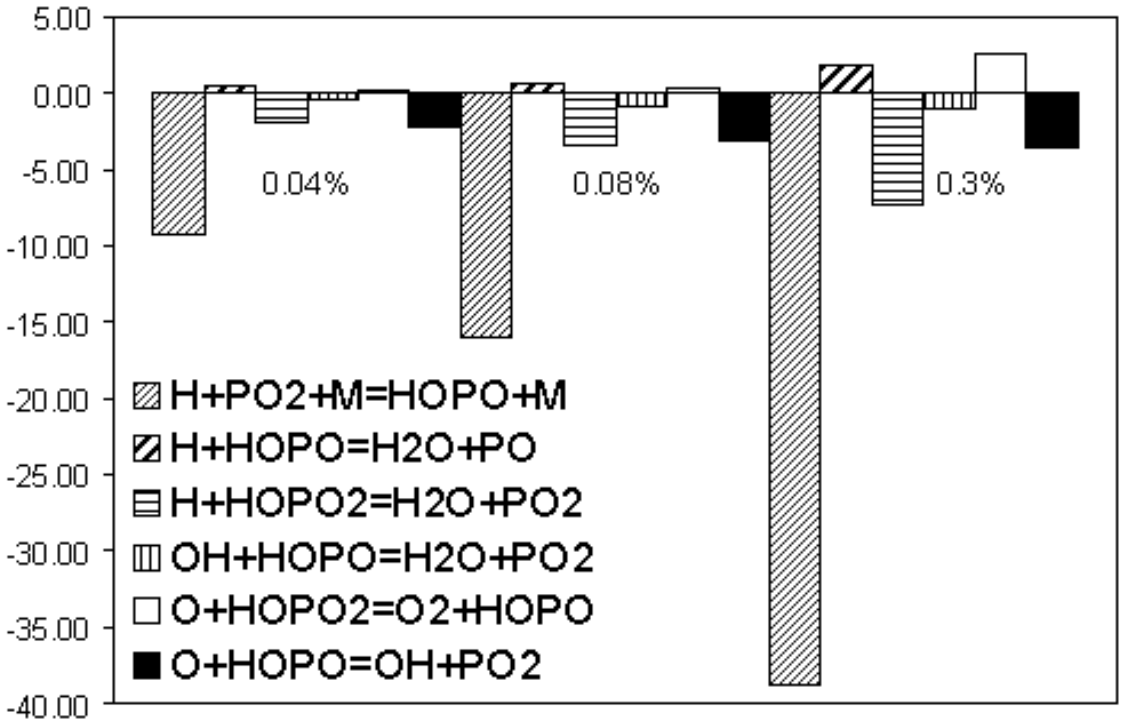

Fig. 31. Influence of varied rate constants of elementary reactions on calculated value $\xi=100\%\times(u-u(k/5))/u$ for our mechanism, where u- burning velocity in stoichiometric CH_4/air mixture doped with TMP of different concentrations at 1 bar, u(k/5) – burning velocity for the rate constants decreased in 5 times.